



The bipartite structure of treatment-trial networks reveals the flow of information in network meta-analysis

Annabel Davies ^{1,*}

¹Bristol Medical School, University of Bristol, Canynge Hall, 39 Whatley Road, BS8 2PS, Bristol, UK

*Corresponding author. annabel.davies@bristol.ac.uk

Abstract

Network meta-analysis (NMA) combines evidence from multiple trials comparing treatment options for the same condition. The method derives its name from a graphical representation of the data where nodes are treatments, and edges represent comparisons between treatments in trials. However, edges in this graph are limited to pairwise comparisons and fail to represent trials that compare more than two treatments. In this paper, we describe NMA as a bipartite graph where trials define a second type of node. Edges then correspond to the arms of trials, connecting each trial node to the treatment nodes it compares. We consider an NMA model parameterized in terms of the observations in each arm. By linking the hat matrix of this model to the bipartite framework, we reveal how evidence flows through the arms of trials. We then define a random walk on the bipartite graph and propose two conjectures that relate the movement of this walker to evidence flow. We illustrate our methods on a network of treatments for plaque psoriasis and verify our conjectures in simulations on randomly generated graphs. The bipartite framework provides new insights into the evidence structure of NMA and the role of individual trials in producing NMA estimates.

Key words: bipartite graph, evidence flow, higher-order interaction, network meta-analysis, random walk

1. Introduction

Network meta-analysis (NMA) is a statistical method widely used in medical research to synthesize evidence from multiple trials that compare treatment options for the same condition (Higgins and Whitehead [1996], Lu and Ades [2004], Dias et al. [2011]). By combining direct and indirect evidence from all relevant trials, NMA produces a coherent ranking of the treatments that allows every intervention to be compared with every other. The results of these analyses are used routinely by policy makers to inform treatment recommendations for clinical practice (Dias et al. [2018]).

The use of indirect evidence in NMA facilitates comparisons between treatments that have never been directly compared in a trial. For example, consider two treatments a and b that have each been compared with a common third treatment c but have not been directly compared with each other. Indirect evidence refers to the idea that we can infer the relationship between a and b via their relations to the common comparator c . That is, if we know that a is more effective than c (from trials comparing a to c) and that c is more effective than b (from trials comparing b to c), then we can infer that a is more effective than b , and by how much.

The evidence structure of an NMA is typically represented as a graph (or network), where nodes are the different treatment options, and the connecting edges represent comparisons between treatments in trials (Lumley [2002]).

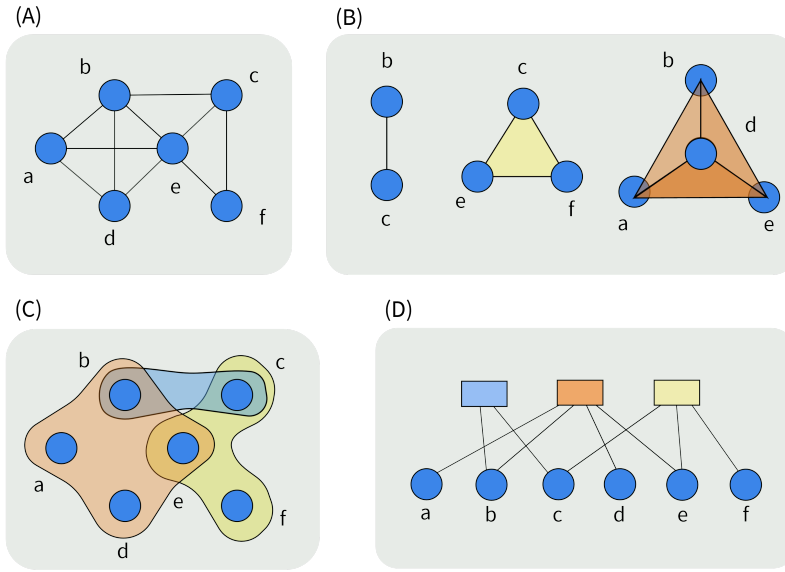


Fig. 1: Four representations of an NMA involving six treatments $[a, b, c, d, e, f]$ compared in three trials; a two-arm trial $[b, c]$, a three arm trial $[c, e, f]$, and a four-arm trial $[a, b, d, e]$. Panel (A) is a graph where treatments are nodes and edges represent pairwise connections between nodes. Each trial introduces a clique (fully connected subgraph) between the treatments it compares. Panel (B) shows three simplicial complexes (with dimensions 1, 2 and 3) representing the three trials. Panel (C) is a hypergraph where hyper-edges represent trials connecting two or more nodes at once. Finally, panel (D) shows a bipartite graph where trials define a second type of node shown as rectangles. Edges represent the arms of a trial, connecting each trial node to the treatment nodes it compares.

The set of treatments compared in a trial are referred to as the arms of the trial. For example, consider a set of six treatments $[a, b, c, d, e, f]$ compared in three trials; a two-arm trial comparing treatments b and c , a three-arm trial comparing c, e , and f , and a four-arm trial comparing a, b, d , and e . Figure 1 (A) shows the graphical representation of this data. An edge connecting two nodes indicates that these treatments have been directly compared in at least one trial. Indirect evidence between pairs of treatments is indicated by connections via intermediate nodes. For example, there is no trial that involves both treatments d and f so these nodes are not connected by an edge. Instead, the comparison between d and f is informed indirectly via intermediate comparisons to treatment e shown by the two edges connecting d to e and e to f . As shown in the Figure, these treatments are also connected via longer paths of indirect evidence involving multiple intermediate nodes.

The network structure of treatment and trials is by no means unique. Similar structures are found in a wide variety of systems; the human brain can be modelled as a network of neurons connected by synapses (Sporns [2002]); networks of roads, railways, and tram lines form the infrastructure of cities across the globe (Gastner and Newman [2006], Sen et al. [2003]); food webs map the interactions between different species in an ecosystem (Krause et al. [2003]); and people in society are connected by friendships, family relationships, and professional collaborations (Zachary [1976], Newman [2001a]). Network structures have long been studied in the related disciplines of graph theory (in mathematics) and complex networks (in statistical physics). Together with the application to various real world systems, these disciplines form the broader field of network science.

Key topics in network science include the identification of influential nodes or edges (Bonacich [1987]), the robustness of networks to the removal of certain components (Albert et al. [2000]), the flow of information through the network (Liben-Nowell and Kleinberg [2008]), and the processes by which nodes become connected as the network is formed (Erdos and Renyi [1960], Barabasi and Albert [1999]). Many of these topics are also relevant for NMA. For example, understanding how evidence from different trials combines to give overall estimates of

treatment effects is a key challenge for NMA. Some trials may lack internal or external validity that mean they provide biased evidence to the network. Understanding how the results of the NMA rely on these trials helps policy-makers to assess how confident they can be in the analysis so that they can make informed decisions and recommendations. Previously, König et al. [2013] defined the ‘flow of evidence’ through the edges of the NMA graph. This visualises how the direct estimates associated with each edge combine to give the overall network estimates. In subsequent work, Papakonstantinou et al. [2018] used these flows to characterise the contributions of different direct and indirect paths of evidence, while Davies et al. [2022] gave an interpretation for evidence flow in terms of the movement of a random walker on the graph.

Characterising the flow of information in NMA is made more challenging by the presence of trials that compare more than two treatments. To include multi-arm trials in the NMA graph, we must first decompose them into their pairwise components. Each n -armed trial then introduces a clique (fully connected subgraph) with $n(n-1)/2$ edges connecting every treatment node in that trial to every other. The resulting graph shows which treatments have been directly compared, but does not allow us to distinguish which comparisons arise from multi-arm trials rather than two-arm trials. For example, from Figure 1 (A) it is impossible to determine whether the edge $[a, e]$ originated from a 2-arm trial between a and e , a 3-arm trial $[a, b, e]$ or $[a, d, e]$, or the (true) 4-arm trial $[a, b, d, e]$. Because we cannot identify individual trials from the edges of the graph, it is not clear how the flow of information through the graph is related to the influence of these trials.

In the language of network science, edges in a graph represent ‘interactions’ between pairs of nodes. More specifically, they represent ‘first order’ interactions. The order of an interaction refers to the number of nodes it involves; an interaction between n nodes has order $n-1$. Orders greater than one (involving more than two nodes) are described as ‘higher-order’. Therefore, multi-arm trials in NMA correspond to higher-order interactions (HOI) in network science; a three-arm trial is a second-order interaction, a four-arm trial is a third-order interaction, and so-on. To accurately describe these trials, we require a higher-order representation that encodes connections between more than two nodes at once.

Panels (B)-(D) in Figure 1 show three HOI representations of our example NMA. In panel (B) each trial is shown as a simplex, a mathematical structure, similar to the concept of a clique, that involves a collection of fully connected nodes. The dimension of a simplex is equivalent to the order of an interaction; the two-arm trial $[b, c]$ is represented by a 1-simplex shown as a line connecting the two nodes, the three arm trial $[c, e, f]$ is a 2-simplex or triangle, and the four-arm trial $[a, b, d, e]$ is a 3-dimensional tetrahedron. A simplicial complex is a collection of simplices involving a set of common nodes that satisfies the condition of ‘downward closure’. This condition requires that if an interaction exists between n nodes, then every possible sub-interaction between these nodes must also exist. For NMA, this means that if, for example, a network includes the three-arm trial $[c, e, f]$ then it must also include the two arm trials $[c, e]$, $[c, f]$, and $[e, f]$, and single arm trials of c , e , and f alone. Since this condition is rarely (if ever) met in practice, simplicial complexes are not a suitable representation of treatment-trial networks.

Another, more flexible representation of HOIs is a hypergraph, shown in panel (C) of Figure 1. A hypergraph is a generalisation of a graph where edges can connect any number of nodes at once. In the context of NMA, an n -armed trial corresponds to a hyperedge connecting n nodes. From Figure 1 (C), it is then immediately clear that the connection between treatments a and e , for example, originates from a 4-arm trial also involving treatments b and d .

Alternatively, hypergraphs can be represented as bipartite structures where the hyperedges (interactions) define a second type of node (Walsh [1975]). Panel (D) in Figure 1 shows the bipartite graph of our example NMA. Here, trials correspond to ‘top nodes’ shown as rectangles and plotted above the circular treatment nodes, now referred to as ‘bottom nodes’. In this representation, edges correspond to the arms of a trial, connecting each trial node to the treatments it compares. Many systems studied in network science have a naturally bipartite structure with the original nodes depicted as bottom nodes, and interactions represented as top nodes (Guillaume and Latapy [2006]). For example, Newman [2001a,b] studied a collaboration network of scientists who are connected if they are co-authors on an academic paper. This naturally maps to a bipartite structure with scientists as the bottom nodes and papers as top nodes. Scientist nodes are then connected to the papers they authored. Similar structures include networks of actors (bottom nodes) and the films (top nodes) in which they co-star (Watts and Strogatz [1998]), or co-occurrence networks of words (bottom nodes) connected by the sentences (top nodes) in which they appear (Solé et al. [2001]).

The bipartite structure of treatment-trial networks and its potential insights have been noted recently (Davies and Galla [2022], Lumley [2024]), but have yet to be explored in practice. In this article, we formalise the bipartite framework for NMA and use this to examine the flow of information through the network. This goes beyond previous work on this topic by revealing how evidence flows through the arms of trials.

The paper is structured as follows: In Section 2 we introduce a motivating NMA dataset of treatments for plaque psoriasis and show its representation both as a graph and a bipartite graph. Section 3 then describes three equivalent formulations of the frequentist NMA model: the standard ‘trial-level’ model written in terms of the relative effects in each trial, an ‘arm-level’ model based on the observations in each arm, and an ‘aggregate’ model that performs the inference in two steps. Each model is expressed as a linear equation with a hat matrix containing the corresponding linear regression coefficients. The mathematical notation describing NMA as a graph, hypergraph and bipartite graph is set out in Section 4. In Section 5, we demonstrate how linking the hat matrices of the different models to the different graphical representations of NMA reveals the flow of information through the network. In particular, we link the arm-level hat matrix to the bipartite graph and use this connection to visualize evidence flow through each trial arm. Finally, we construct a random walk on the bipartite graph and propose two conjectures that relate the walker’s movement to evidence flow. In Section 6 we apply our approach to the motivating example, and in Section 7 we verify our conjectures on simulated datasets. Finally, we summarize and discuss our work in Section 8.

2. Motivating dataset

We consider a dataset from Warren et al. [2018] comparing seven treatments for plaque psoriasis. The network includes nine trials; three are four-arm trials, four are three-arm, and two have just two arms. The outcome of interest we focus on is an improvement of 75% on the Psoriasis Area and Severity Index (PASI) scale at 12 weeks compared to baseline. We measure the treatment effect in each arm as the log odds of achieving this outcome. The relative treatment effect is a log odds ratio. The dataset is available to download from the *multinma* package in R (Phillippo [2024]).

The graph corresponding to this data is shown in Figure 2 (A) and comprises 7 nodes representing the treatments and 13 edges representing pairwise comparisons. The thickness of each edge is proportional to the number of trials that have made that comparison. From this figure, we can see which treatments have been directly compared but we cannot tell which comparisons come from multi-arm trials. In contrast, the bipartite graph in Figure 2 (B) shows precisely which treatments are compared in each trial. This graph comprises 16 nodes; 9 top nodes representing the trials, and 7 bottom nodes representing the treatments. There are 28 edges representing the arms of the trials. The number of edges connected to a node is referred to as its ‘degree’. The degree of a trial node corresponds to

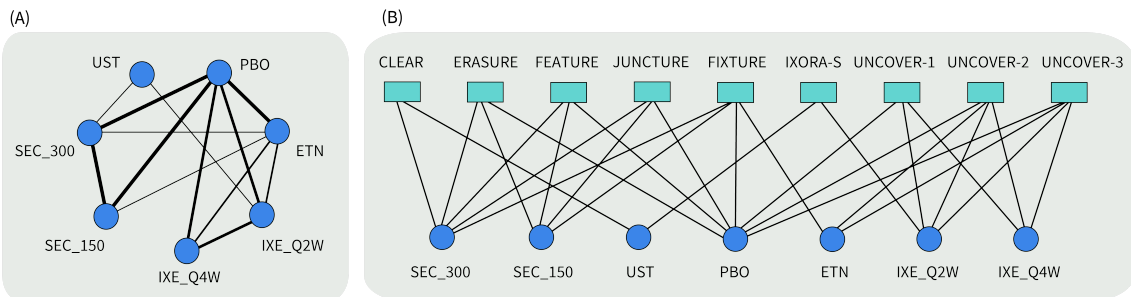


Fig. 2: (A) A graph representing the plaque psoriasis NMA. Each node represents a treatment, and two nodes are connected by an edge if they have been compared in at least one trial. The thickness of each edge is proportional to the number of trials comparing those two treatments. Treatments are labelled as follows: PBO, placebo; IXE, ixekizumab; SEC, secukinumab; ETN, etanercept; UST, ustekinumab. IXE and SEC were each investigated with 2 different dosing regimens. (B) A bipartite graph representing the same dataset. Bottom nodes (circles) represent the same set of treatments as in (A) and top nodes (squares) represent trials. Trial nodes are connected to the treatment nodes they compare. Trial labels correspond to the names assigned in Warren et al. [2018].

the number arms in that trial, whereas the degree of the treatment node tells us the number of trials in which that treatment appeared. For example, the degree of the JUNCTURE trial node is three, representing the three treatments in that trial; two doses of secukinumab (SEC_150 and SEC_300) and a placebo (PBO). The degree of the UST treatment node is two, meaning this treatment only appears in two trials (CLEAR and IXORA-S).

Performing an NMA on this dataset reveals the relative effects between each pair of treatments in the network. Of particular clinical interest is the comparison between the licensed doses of interleukin-17 blockers, secukinumab 300mg (SEC_300) and ixekizumab every 2 weeks (IXE_Q2W). To make an informed decision between these treatments, policy makers need to know which trials form the main evidence base for the comparison. A key step to achieving this is understanding how information or ‘evidence’ flows through the network.

3. NMA models

In this section, we introduce three parameterisations of the frequentist inverse-variance NMA model. Each parameterisation is expressed as a linear model that regresses the trial observations on a set of consistent treatment effects. The influence of observations from the different trials is related to the structure of the network and the (inverse-variance) weight assigned to each observation in the model. This information is captured in the model’s hat matrix which contains the linear regression coefficients.

3.1. Set-up and notation

We consider a network of N treatments, labelled $j = 1, \dots, N$, that are compared in M trials, $i = 1, \dots, M$. Each trial i compares a subset of n_i treatments, $\mathcal{T}_i = [t_{i\ell}; \ell = 1, \dots, n_i] \subset [1, \dots, N]$, each associated with an observed mean $\mu_{i,t_{i\ell}}$ and variance $\sigma_{i,t_{i\ell}}^2$. We define relative treatment effects, or ‘contrasts’, with reference to some trial-specific baseline treatment t_{i1} . Each trial is then associated with $n_i - 1$ contrast-level observations comparing each arm $t_{i\ell \neq 1}$ to the baseline,

$$y_{i,t_{i1}t_{i\ell}} = \mu_{i,t_{i\ell}} - \mu_{i,t_{i1}}. \quad (1)$$

Collecting the arm- and contrast-level observations into the vectors $\boldsymbol{\mu}$ and \boldsymbol{y} respectively, we can write Equation (1) as

$$\boldsymbol{y} = \boldsymbol{C}\boldsymbol{\mu}, \quad (2)$$

where the matrix \boldsymbol{C} maps the arm-level observations in each trial onto the contrast-level. Each trial contributes an $(n_i - 1) \times n_i$ block matrix \boldsymbol{C}_{n_i} whose columns represent the arms of the trial and rows represent comparisons to the baseline t_{i1} . In each row, the element corresponding to t_{i1} is equal to -1 and the element corresponding to $t_{i\ell}$ is $+1$. In other words, $\boldsymbol{C}_{n_i} = [-\mathbf{1}_{n_i-1} \quad \boldsymbol{I}_{n_i-1}]$ where $\mathbf{1}_{n_i-1}$ is an $(n_i - 1)$ -column vector of ones and \boldsymbol{I}_{n_i-1} is the $(n_i - 1) \times (n_i - 1)$ identity matrix. These blocks are arranged diagonally in \boldsymbol{C} , with the remaining elements equal to zero.¹ We show an example of this matrix in Section 5.2.1.

The covariance matrix describing the sampling variances and correlations of the contrast-level observations is a block diagonal, $\boldsymbol{\Sigma} = \text{diag}(\boldsymbol{\Sigma}_1, \dots, \boldsymbol{\Sigma}_M)$. Each trial i contributes an $(n_i - 1) \times (n_i - 1)$ matrix $\boldsymbol{\Sigma}_i$ with diagonal elements equal to the variance of each $y_{i,t_{i1}t_{i\ell}}$. Assuming the arms are independent, these elements are equal to the sum of the arm-level variances, $v_{i,t_{i1}t_{i\ell}} = \sigma_{i,t_{i1}}^2 + \sigma_{i,t_{i\ell}}^2$. The off-diagonal elements are the covariances between each pair of contrast-level observations, $\text{cov}(y_{i,t_{i1}t_{i\ell}}, y_{i,t_{i1}t_{i\ell'}})$, equal to the variance in the baseline arm of that trial, $\sigma_{i,t_{i1}}^2$.

3.2. Model assumptions

We write θ_{jk} for the mean relative treatment effect between treatments j and k . We adopt the convention $\theta_{jk} = -\theta_{kj}$ and $\theta_{jj} = 0$. We also make the usual assumption that for any treatments j, k and l , the relative treatment effects

¹ Formally, \boldsymbol{C} is a direct sum of the trial-level blocks, $\boldsymbol{C} = \boldsymbol{C}_{n_1} \oplus \boldsymbol{C}_{n_2} \oplus \dots \oplus \boldsymbol{C}_{n_M}$.

fulfill the consistency (transitivity) relation,

$$\theta_{jk} = \theta_{lk} - \theta_{lj}. \quad (3)$$

Assuming consistency, the relative treatment effects of all N treatments are fully specified by $N-1$ ‘basic’ parameters. That is, if we assign treatment 1 as the ‘global’ baseline, it is sufficient to know θ_{1j} for $j = 2, \dots, N$. We collect the basic parameters in the $(N-1)$ -dimensional vector, θ .

Following the standard inverse-variance model, we assume the contrast-level observations \mathbf{y} are normally distributed about their mean effects such that,

$$\mathbf{y} \sim \mathcal{N}(\mathbf{X}\theta, \mathbf{W}^{-1}), \quad (4)$$

where \mathbf{X} is the design matrix describing which comparisons are made in each trial (see Section A of the Supplement), and \mathbf{W} is the inverse-variance weight matrix. In the common effect (CE) model, $\mathbf{W} = \Sigma^{-1}$. In the random effects (RE) model, we allow the ‘true’ relative treatment effects to vary between trials. We assume trial-specific effects are drawn from a multivariate normal distribution centred on the mean effects $\mathbf{X}\theta$, with between-trial covariance matrix Ω . The RE weight matrix in Equation (4) is then $\mathbf{W} = (\Sigma + \Omega)^{-1}$. For our purposes the form of Ω is not important, but the usual assumption is that all relative effects share a common between-trial heterogeneity variance, τ^2 . The covariance matrix is then a block diagonal $\Omega = \text{diag}(\Omega_1, \dots, \Omega_M)$ where Ω_i has dimensions $(n_i - 1) \times (n_i - 1)$ with diagonal entries equal to τ^2 and off-diagonal entries equal to $\tau^2/2$.

3.3. Trial-level hat matrix

The usual frequentist estimate of the basic parameters is obtained via generalised least-squares regression or, equivalently for model (4), maximum likelihood. The solution is the well-known Aitken estimator (Aitken [1936]),

$$\hat{\theta} = \mathbf{H}\mathbf{y}, \quad (5)$$

where we label \mathbf{H} the ‘trial-level’ hat-matrix, given by

$$\mathbf{H} = (\mathbf{X}'\mathbf{W}\mathbf{X})^{-1}\mathbf{X}'\mathbf{W}, \quad (6)$$

with dimensions $(N-1) \times \sum_{i=1}^M (n_i - 1)$. In Equation (6), we use the notation \mathbf{X}' to indicate the transpose of matrix \mathbf{X} .

Each row of \mathbf{H} contains the coefficients of a linear equation describing how the estimates of each basic parameter, $\hat{\theta}_{1j}$, depend on the contrast-level observations from each trial, $y_{i,t_{11}t_{1j}}$. To obtain the $N(N-1)/2$ relative effects between every pair of treatments, we apply the consistency equations in (3) to the estimates of the basic parameters in Equation (5). Applying these equations to the right hand side of Equation (5) yields the ‘full’ hat matrix containing the coefficients for the full set of relative treatment effects. For example, the coefficients for the relative effect $\hat{\theta}_{jk}$ ($j, k \neq 1$) are obtained by subtracting the row of the hat matrix corresponding to the basic comparison $1j$ from the row corresponding to $1k$,

$$\mathbf{H}^{(jk)} = \mathbf{H}^{(1k)} - \mathbf{H}^{(1j)}. \quad (7)$$

3.4. Arm-level hat matrix

Using the relationship between the contrast-level and arm-level observations, we can instead write the model in terms of the vector of means in each arm μ . Substituting Equation (2) into Equation (5), we obtain

$$\hat{\theta} = \mathbf{H}_{\top\perp}\mu, \quad (8)$$

where we define the arm-level² hat matrix $\mathbf{H}_{\top\perp}$ as a projection of the trial-level hat matrix,

$$\mathbf{H}_{\top\perp} = \mathbf{H}\mathbf{C} = (\mathbf{X}'\mathbf{W}\mathbf{X})^{-1}\mathbf{X}'\mathbf{W}\mathbf{C}, \quad (9)$$

² In the terminology set out by White et al. [2019], the arm-level model we describe is not ‘arm-based’. That is, we apply modeling assumptions to parameters representing relative effects (contrasts) rather than parameters representing arm means. Our model is simply a parameterization of the standard contrast-based model in terms of the arm-level data. This is what White et al. [2019] calls a contrast-based model with an arm-based likelihood.

with dimensions $(N - 1) \times \sum_i n_i$. The use of the notation $\top \perp$ will become apparent in later sections when we connect the hat matrices to the different graphical representations of NMA.

Each row of $H_{\top \perp}$ contains the coefficients of a linear equation describing how the estimates of each basic parameter $\hat{\theta}_{ij}$ depend on the observations in each arm of each trial, $\mu_{i,t_{it}}$. Again, we obtain the coefficients for every pairwise comparison by applying the consistency equations in (7).

3.5. Aggregate hat matrix

Another alternative formulation of the model is to perform the regression in two steps (Lu et al. [2011], Krahn et al. [2013]). In the first step, trials comparing the same treatments are combined to obtain a set of direct estimates. Then, the direct estimates are entered as the observations in an NMA. This is referred to as an ‘aggregate’ model. In particular, we use a ‘graph-theoretical’ version of the aggregate model that accounts for correlations due to multi-arm trials before combining the direct evidence on each pairwise comparison. We describe the model in Section B of the Supplement and refer to Davies et al. [2022] and its Supplementary Materials for further details. The key points are summarized below.

In the first step, we account for correlations by adjusting the variances associated with each comparison in each multi-arm trial. Using these adjusted weights, we then perform a pairwise meta-analysis (weighted mean) for each pair of treatments that have been compared in at least one trial. The resulting direct estimates are collected in the vector $\hat{\theta}^{\text{dir}}$ and their associated weights in the diagonal matrix $W_{\perp} = \text{diag}(w_{jk})$.

In the second step, we perform an NMA using the direct estimates. The network estimates of the $N - 1$ basic parameters are obtained via the linear equation

$$\hat{\theta} = H_{\perp} \hat{\theta}^{\text{dir}}, \quad (10)$$

where we write H_{\perp} for the aggregate hat matrix, defined as

$$H_{\perp} = C_N (B'_{\perp} W_{\perp} B_{\perp})^{+} B'_{\perp} W_{\perp}. \quad (11)$$

The matrix B_{\perp} is an oriented edge-vertex incidence matrix. Each column corresponds to a treatment and each row corresponds to a direct estimate (edge) between two treatments. Without loss of generality, each row representing an edge between treatments j and k is given an arbitrary orientation, with a -1 in column j and $+1$ in column k . All other entries are 0. We return to this matrix in Section 4.1 below. Recall from Section 3.1 the definition of matrix $C_N = [-1_{N-1} \quad I_{N-1}]$. In Equation (11), this matrix ensures that H_{\perp} has the correct dimensions for projecting onto the $N - 1$ basic parameters. Finally, the matrix operation $^{+}$ indicates its Moore-Penrose pseudo-inverse.

The aggregate hat matrix has $(N - 1)$ rows representing the comparison of each treatment to the global baseline. The number of columns is equal to the number of direct estimates (the number of edges in the NMA graph). Each row contains the coefficients of a linear equation describing how the estimates of each basic parameter $\hat{\theta}_{ij}$ depend on the direct estimates associated with each edge. As before, we obtain the full version of the aggregate hat matrix by applying the consistency equations in (7).

4. Network representations

In this section, we set out the mathematical descriptions of the graph, hypergraph and bipartite graph representations of treatments and trials. To keep track of how the notation and terminology in these different frameworks correspond to one another and to concepts in NMA, we provide a summary in Table 1 for the reader to refer back to.

4.1. Graphs

Traditionally, treatments and trials in an NMA are represented as a graph, $G_{\perp} = [V_{\perp}, E_{\perp}]$, where $V_{\perp} = [v_j; j = 1, \dots, N]$ is a set of N nodes representing the treatments and E_{\perp} is a set of K_{\perp} edges connecting pairs of nodes. An edge $[v_j, v_k] \in E_{\perp}$ is defined by the two nodes it connects and is a natural representation of a 2-arm trial. However, to represent multi-arm trials, we must first decompose them into their pairwise components. Each multi-arm trial then introduces a fully connected subgraph, known as a ‘clique’, between the treatment nodes in that trial. For

Table 1. Terminology and notation in NMA and network theory.

NMA	Graph	Hypergraph	Bipartite graph
Treatments $j = 1, \dots, N$	Nodes $V_{\perp} = [v_j]$	Nodes $V_{\perp} = [v_j]$	Bottom nodes $V_{\perp} = [v_j]$
Trials $i = 1, \dots, M$	Cliques ¹	Hyperedges $\mathcal{H} = [\mathcal{H}_i]$	Top nodes $V_{\top} = [u_i]$
Trial arms $\mathcal{T}_i = [t_{i\ell}; \ell = 1, \dots, n_i]$	Edges in a clique ¹ $[[v_{i1}, v_{i2}], \dots, [v_{in_i-1}, v_{in_i}]]$	Nodes connected by $\mathcal{H}_i = [v_{i\ell}; \ell = 1, \dots, n_i]$	Edges connecting u_i to adjacent bottom nodes
n_i , number of arms in trial i	Size of clique	Number of nodes connected by hyperedge \mathcal{H}_i	Degree of top node u_i

¹In a graph, edges represent comparisons between treatments in trials. An n_i -armed trial gives rise to a clique (fully connected subgraph) of size n_i . However, unlike the hypergraph and bipartite graph, there is no 1:1 mapping between a component in the graph and a trial or trial-arm.

instance, returning to our example from the Introduction, the three trials $[b, c]$, $[c, e, f]$, and $[a, b, d, e]$ can be decomposed into the edgeset $E_{\perp} = [[b, c], [c, e], [c, f], [e, f], [a, b], [a, d], [a, e], [b, d], [b, e], [d, e]]$ (shown in panel (A) of Figure 1).

Mathematically, a graph is described by its adjacency matrix A_{\perp} . This is a square $N \times N$ matrix where each row and column represents a node. An element $A_{\perp,jk}$ is equal to 1 if nodes v_j and v_k are connected by an edge, otherwise it is 0. The adjacency matrix of the graph in Figure 1 (A) is

$$A_{\perp} = \begin{matrix} & \begin{matrix} a & b & c & d & e & f \end{matrix} \\ \begin{matrix} a \\ b \\ c \\ d \\ e \\ f \end{matrix} & \begin{pmatrix} 0 & 1 & 0 & 1 & 1 & 0 \\ 1 & 0 & 1 & 1 & 1 & 0 \\ 0 & 1 & 0 & 0 & 1 & 1 \\ 1 & 1 & 0 & 0 & 1 & 0 \\ 1 & 1 & 1 & 1 & 0 & 1 \\ 0 & 0 & 1 & 0 & 1 & 0 \end{pmatrix} \end{matrix}, \quad (12)$$

where we have labelled the rows and columns by the nodes they represent. The sum of the entries in each row and column of A_{\perp} is equal to the degree of that node. For example, the entries of row c and column c each sum to 3 which corresponds to the number of edges connected to node c in Figure 1 (A). As we will see later, for weighted graphs, one can define a weighted adjacency matrix where each element $A_{\perp,jk}$ is equal to the weight associated with the edge $[v_j, v_k]$. The weighted degree of a node is then the sum of weights in the edges connected to that node.

A graph can also be described by its incidence matrix B_{\perp} which encodes relationships between nodes and edges. We focus on the $K_{\perp} \times N$ edge-vertex incidence matrix where each row represents an edge $e \in E_{\perp}$ and each column represents a node $v \in V_{\perp}$.² The elements of B_{\perp} are defined such that the row representing edge $[v_j, v_k]$ contains a 1

² In network theory, one often comes across the $N \times K_{\perp}$ vertex-edge incidence matrix which is the transpose of the edge-vertex incidence matrix. Both matrices may be referred to as simply the ‘incidence matrix’ so care must be taken to understand the definition being used in any given context. Throughout this article we will define all incidence matrices in their edge-vertex orientation.

in both columns j and k . All other entries are zero. For our example, we have

$$\mathbf{B}_\perp = \begin{matrix} & \begin{matrix} a & b & c & d & e & f \end{matrix} \\ \begin{matrix} [b, c] \\ [c, e] \\ [c, f] \\ [e, f] \\ [a, b] \\ [a, d] \\ [a, e] \\ [b, d] \\ [b, e] \\ [d, e] \end{matrix} & \begin{pmatrix} 0 & 1 & 1 & 0 & 0 & 0 \\ 0 & 0 & 1 & 0 & 1 & 0 \\ 0 & 0 & 1 & 0 & 0 & 1 \\ 0 & 0 & 0 & 0 & 1 & 1 \\ 1 & 1 & 0 & 0 & 0 & 0 \\ 1 & 0 & 0 & 1 & 0 & 0 \\ 1 & 0 & 0 & 0 & 0 & 1 \\ 0 & 1 & 0 & 1 & 0 & 0 \\ 0 & 1 & 0 & 0 & 1 & 0 \\ 0 & 0 & 0 & 1 & 1 & 0 \end{pmatrix} \end{matrix}, \quad (13)$$

where the sum of elements in each row is 2 and the sum of elements in each column is the degree of the node it represents. The matrix in (13) is an unoriented incidence matrix describing undirected edges. For a directed network, we can instead define an oriented version where an edge directed from v_j to v_k has a -1 in column j and a $+1$ in column k . Each row then sums to 0. It is this oriented version of the edge-vertex incidence matrix that appears in the definition of the aggregate hat matrix in Equation (11).

The benefit of representing NMA as a graph is that it allows us to use the many well-established tools and techniques from graph theory. However, by encoding only pairwise connections, the graph fails to accurately represent multi-arm trials.

4.2. Hypergraphs

Hypergraphs offer the most flexible representation of higher-order interactions and therefore, provide an accurate description of multi-arm trials in NMA. A hypergraph $G_{\mathcal{H}} = [V_\perp, \mathcal{H}]$ is a generalisation of a graph, defined by the original nodeset V_\perp and a set of hyperedges $\mathcal{H} = [\mathcal{H}_i]$ that connect groups of nodes. Unlike an edge in a graph, which represents a pairwise connection, a hyperedge can connect any number of nodes in V_\perp . A hyperedge is defined by the subset of nodes it connects, $\mathcal{H}_i = [v_{i\ell}; \ell = 1, \dots, n_i]$, and therefore corresponds naturally to a trial comparing n_i treatments.

An adjacency matrix tells us whether two nodes are connected but does not provide any information about the edge from which the connection derives. To fully describe a hypergraph therefore requires an incidence matrix, \mathbf{B} . Similar to the incidence matrix of the graph, columns of \mathbf{B} represent nodes $\in V_\perp$ while rows represent hyperedges $\in \mathcal{H}$. For the row representing hyperedge \mathcal{H}_i , the element B_{ij} is equal to 1 if node v_j is connected to that hyperedge ($v_j \in \mathcal{H}_i$) and is 0 otherwise. The incidence matrix of the hypergraph in Figure 1 (C) is therefore

$$\mathbf{B} = \begin{matrix} & \begin{matrix} a & b & c & d & e & f \end{matrix} \\ \begin{matrix} \mathcal{H}_1 \\ \mathcal{H}_2 \\ \mathcal{H}_3 \end{matrix} & \begin{pmatrix} 0 & 1 & 1 & 0 & 0 & 0 \\ 0 & 0 & 1 & 0 & 1 & 1 \\ 1 & 1 & 0 & 1 & 1 & 0 \end{pmatrix} \end{matrix}, \quad (14)$$

where $\mathcal{H}_1 = [b, c]$, $\mathcal{H}_2 = [c, e, f]$, and $\mathcal{H}_3 = [a, b, d, e]$. Here, the elements in each row sum to the number of nodes connected by that hyperedge and each column sums to the number of hyperedges connected to that node (known as the hyper-degree of the node).

Although many concepts and results from graph theory can be extended to hypergraphs, this often comes with increased mathematical complexity. For NMA, this is compounded by the fact that we often have multiple trials that have compared the same set of treatments. This requires a so-called ‘multi-hypergraph’ which allows multiple hyperedges to connect the same set of nodes. This is known as ‘edge-multiplicity’ and further increases the complexity of these structures.

4.3. Bipartite graphs

A bipartite graph $G_{\top\perp} = [V_{\top}, V_{\perp}, E_{\top\perp}]$ contains two disjoint sets of nodes, V_{\top} and V_{\perp} , referred to as the top and bottom nodes respectively. $E_{\top\perp} \subseteq V_{\top} \times V_{\perp}$ defines a set of edges connecting pairs of nodes of opposite types. The structure is such that edges only exist between top and bottom nodes; there can be no edge between two top nodes or between two bottom nodes. The terminology derives from the standard visualization of bipartite graphs where the two sets of nodes are arranged in two horizontal lines, with top nodes appearing above bottom nodes.

Hypergraphs can be represented as bipartite structures where bottom nodes are the original node set V_{\perp} , top nodes correspond to the hyperedges $V_{\top} = \mathcal{H}$, and edges capture pairwise connections between nodes and hyperedges. We retain the notation v_j ($j = 1, \dots, N$) to label bottom nodes, and write u_i ($i = 1, \dots, M$) for top nodes such that node u_i corresponds to the hyperedge \mathcal{H}_i . We write $[u_i, v_j]$ for the edge connecting top node u_i to bottom node v_j . In NMA, the bottom nodes are treatments and top nodes are trials. Edges then represent the arms of a trial, connecting trial nodes to the treatment nodes they compare. The degree of a trial node is equal to the number of arms in that trial, while the degree of a treatment node tells us the number of trials that treatment is involved in.

By representing interactions themselves as nodes, the bipartite framework re-establishes edges as encoding pairwise connections. This means that we can describe the bipartite graph using an adjacency matrix A that tells us whether or not two nodes are connected. Given M top nodes and N bottom nodes, the adjacency matrix of the bipartite graph has dimensions $(M + N) \times (M + N)$. The first M rows and columns represent the top nodes (trials) and the final N rows and columns represent the bottom nodes (treatments). As before, an element of A is equal to 1 if the nodes corresponding to that row and column are connected, and is 0 otherwise. For the example in Figure 1 (D), we find

$$A = \begin{matrix} & \begin{matrix} u_1 & u_2 & u_3 & a & b & c & d & e & f \end{matrix} \\ \begin{matrix} u_1 \\ u_2 \\ u_3 \\ a \\ b \\ c \\ d \\ e \\ f \end{matrix} & \begin{pmatrix} 0 & 0 & 0 & 0 & 1 & 1 & 0 & 0 & 0 \\ 0 & 0 & 0 & 0 & 0 & 1 & 0 & 1 & 1 \\ 0 & 0 & 0 & 1 & 1 & 0 & 1 & 1 & 0 \\ 0 & 0 & 1 & 0 & 0 & 0 & 0 & 0 & 0 \\ 1 & 0 & 1 & 0 & 0 & 0 & 0 & 0 & 0 \\ 1 & 1 & 0 & 0 & 0 & 0 & 0 & 0 & 0 \\ 0 & 0 & 1 & 0 & 0 & 0 & 0 & 0 & 0 \\ 0 & 1 & 1 & 0 & 0 & 0 & 0 & 0 & 0 \\ 0 & 1 & 0 & 0 & 0 & 0 & 0 & 0 & 0 \end{pmatrix} \end{matrix}, \quad (15)$$

where $u_1 = [b, c]$, $u_2 = [c, e, f]$, and $u_3 = [a, b, d, e]$. Equation (15) reveals a block diagonal structure that is characteristic of the adjacency matrices of bipartite graphs. Because two nodes of the same type cannot be connected, the $M \times M$ and $N \times N$ diagonal blocks representing connections between pairs of top nodes and between pairs of bottom nodes are equal to zero. On inspection, we observe that the $M \times N$ upper right block is equal to the incidence matrix of the hypergraph in Equation (14). The $N \times M$ lower left block is equal to its transpose, B' . The adjacency matrix therefore takes the form

$$A = \begin{pmatrix} 0 & B \\ B' & 0 \end{pmatrix}. \quad (16)$$

In the bipartite framework, the matrix B is referred to as the ‘biadjacency matrix’ and encodes all the information about the graph. Therefore, it is often the biadjacency matrix rather than the full adjacency matrix A that is used to describe bipartite graphs.

It can also be useful to define the edge-vertex incidence matrix of the bipartite graph. To distinguish this from the biadjacency matrix, we label it $B_{\top\perp}$. It is defined in the same way as the incidence matrix of a graph, with rows representing edges $\in E_{\top\perp}$ (trial arms), and columns representing nodes. The first M columns correspond to top nodes $\in V_{\top}$ (trials) and the last N columns correspond to bottom nodes $\in V_{\perp}$ (treatments). For the row representing edge $[u_i, v_j]$ there is a 1 in both columns i and $i + j$. All other entries are 0. As before, an oriented version of the

Table 2. A summary of notation for the three different types of graph.

	Graph	Hypergraph	Bipartite graph
Graph	G_{\perp}	$G_{\mathcal{H}}$	$G_{\top\perp}$
Nodeset	V_{\perp}	V_{\perp}	$[V_{\top}, V_{\perp}]$
Edgeset	$E_{\perp} \subseteq V_{\perp} \times V_{\perp}$	\mathcal{H}	$E_{\top\perp} \subseteq V_{\top} \times V_{\perp}$
Node	$v_j \in V_{\perp}$	$v_j \in V_{\perp}$	$u_i \in V_{\top}, v_j \in V_{\perp}$
Edge	$[v_j, v_k]$	$[v_j, v_k, v_l, \dots]$	$[u_i, v_j]$
Number of nodes	N	N	$M + N$
Number of edges	K_{\perp}	M	$K_{\top\perp}$
Adjacency matrix	A_{\perp}	-	$A = \begin{pmatrix} 0 & B \\ B' & 0 \end{pmatrix}$
Incidence matrix	B_{\perp}	B	$B_{\top\perp}$

incidence matrix can be defined by setting the element in column i equal to -1 . In Section C of the Supplement, we show $B_{\top\perp}$ for the example in Figure 1 (D). We summarize our notation in Table 2.

The relation in Equation (16) reveals the 1:1 mapping between hypergraphs and bipartite graphs. Despite this equivalence, the two representations have different mathematical properties. By encoding only pairwise connections between nodes, bipartite graphs more easily inherit operations and results from standard graph theory. Moreover, the bipartite framework naturally facilitates hyperedge multiplicity; multiple top nodes may connect the same set of bottom nodes without introducing any additional complexity. For these reasons, we select bipartite graphs as the most useful representation of higher-order structures in NMA networks.

4.3.1. Unipartite projection

The unipartite graph $G_{\perp} = (V_{\perp}, E_{\perp})$ associated with the bipartite graph $G_{\top\perp} = (V_{\top}, V_{\perp}, E_{\top\perp})$ is called the unipartite-projection of $G_{\top\perp}$. Throughout the remainder of the article, we will use the term ‘unipartite graph’ to distinguish it from the bipartite graph. Other terminology includes the one-mode-, clique-based, bottom-, or \perp -projection (Guillaume and Latapy [2004]). In this projection, edge $[v_j, v_k]$ is in E_{\perp} if bottom nodes v_j and v_k are both connected to the same top node in $G_{\top\perp}$. Therefore, each top node in $G_{\top\perp}$ induces a clique in G_{\perp} between the bottom nodes to which it is linked. For example, in Figure 1, the graph in panel (A) is the unipartite-projection of the bipartite graph in panel (D). The central top node in panel (D) is connected to four bottom nodes a, b, d, e . In panel (A) this corresponds to the fully connected subgraph linking each pair of these nodes to each other.

Every bipartite graph corresponds to a unique unipartite-projection. However, the reverse does not hold: a single unipartite projection can result from multiple distinct bipartite graphs. In general, therefore, it is not possible to reconstruct the original bipartite graph from a given unipartite graph. Indeed, this is the problem we described earlier that means we cannot identify multi-arm trials from the unipartite representation of NMA.

5. Flow of information

In this section we explore the flow of information through the network by linking the different hat matrices in Section 3 to the different network representations in Section 4. We begin with a review of previous work connecting the aggregate hat matrix to evidence flow on the unipartite graph. We present a theorem relating this evidence flow to the movement of a random walker on the graph. Building on these previous results, we link the arm-level hat matrix to the bipartite graph and use this connection to visualize evidence flow through each trial arm. Finally, we construct a higher order random walk on the bipartite graph and propose two conjectures that relate the walker’s movement to evidence flow across both the bipartite and unipartite graphs.

5.1. Unipartite evidence flow

5.1.1. The aggregate hat matrix

The aggregate hat matrix \mathbf{H}_\perp contains the coefficients of a linear equation relating the treatment effect estimates to the direct estimates. Each direct estimate is associated with an edge in the unipartite NMA graph. König et al. [2013] showed that each row of \mathbf{H}_\perp representing a particular treatment comparison jk describes a directed network from node v_j to node v_k on this graph. Each element of the row corresponds to an edge $[v_l, v_m] \in E_\perp$. The magnitude of flow between nodes v_l and v_m is given by the absolute value of this element and the direction of flow is determined by its sign. We refer to König et al. [2013], Davies et al. [2022], and Rücker et al. [2024] for a discussion of the properties of these flow networks.

As an illustration, we consider a fictional example with $M = 5$ trials labelled $[1, 2, 3, 4, 5]$, and $N = 4$ treatments labelled $[a, b, c, d]$. The network contains three two-armed trials (1, 3, and 5) and two three-armed trials (2 and 4). Table 3 shows the arm-level data associated with each trial.

Table 3. Arm level data for our fictional example network.

Trial, i	Arms, $\mathcal{T}_i = [t_{i\ell}]$	Means, $[\mu_{i,t_{i\ell}}]$	Variances, $[\sigma_{i,t_{i\ell}}^2]$
1	$[a, b]$	$[1.0, 2.0]$	$[0.2, 0.3]$
2	$[a, b, c]$	$[0.8, 2.1, 1.5]$	$[0.4, 0.6, 0.5]$
3	$[a, d]$	$[1.2, 1.5]$	$[0.8, 0.9]$
4	$[b, c, d]$	$[2.0, 1.6, 1.2]$	$[1.2, 1.1, 1.0]$
5	$[c, d]$	$[1.4, 0.9]$	$[0.5, 0.4]$

We assume a CE model ($\tau = 0$), and choose treatment a as the global baseline. Panel (A) of Figure 3 shows the unipartite graph of this example. The graph has $K_\perp = 6$ edges, $E_\perp = [[a, b], [a, c], [a, d], [b, c], [b, d], [c, d]]$, with weights $\mathbf{W}_\perp = \text{diag}(2.676, 0.811, 0.588, 0.817, 0.304, 1.443)$. Following the convention set out in Section 3.5, the oriented incidence matrix of this graph is

$$\mathbf{B}_\perp = \begin{pmatrix} -1 & 1 & 0 & 0 \\ -1 & 0 & 1 & 0 \\ -1 & 0 & 0 & 1 \\ 0 & -1 & 1 & 0 \\ 0 & -1 & 0 & 1 \\ 0 & 0 & -1 & 1 \end{pmatrix}. \quad (17)$$

Substituting these matrices into Equation (11) gives the aggregate hat matrix,

$$\mathbf{H}_\perp = \begin{pmatrix} 0.812 & 0.113 & 0.074 & -0.134 & -0.054 & -0.020 \\ 0.375 & 0.424 & 0.201 & 0.313 & 0.061 & -0.262 \\ 0.337 & 0.277 & 0.386 & 0.176 & 0.161 & 0.453 \end{pmatrix}, \quad (18)$$

where each column corresponds to an edge $\in E_\perp$ and each row represents a comparison with the baseline treatment; ab, ac , and ad .

The first row of \mathbf{H}_\perp in Equation (18) corresponds to the comparison ab and defines an evidence flow network from node a to node b , shown in panel (B) of Figure 3. The thickness of each edge is proportional to the magnitude of the coefficient associated with that edge and the direction is given by its sign. For example, the final element of the row represents edge $[c, d]$. The magnitude of flow through this edge is 0.02 and the negative sign indicates that evidence flows in the direction from d to c . In Figure 3 (B) we observe the greatest flow along the edge from a to b . This indicates that the direct evidence on ab , $\hat{\theta}_{ab}^{\text{dir}}$, has the largest coefficient in the linear equation for $\hat{\theta}_{ab}$ and therefore contributes the most to the network estimate.

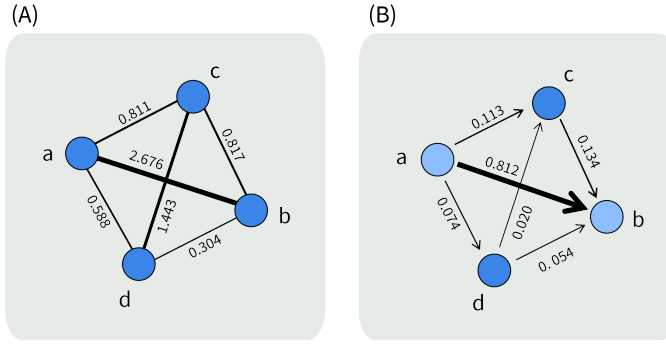


Fig. 3: (A) Weighted unipartite graph for the fictional example network described in Table 3. The thickness of each edge $[v_j, v_k]$ is proportional to its aggregate weight w_{jk} in the corresponding element of $\mathbf{W}_\perp = \text{diag}(w_{jk})$. These weights are shown in the edge labels. (B) The evidence flow network for the comparison of treatments a and b . The thickness of each edge is proportional to the corresponding element of the aggregate hat matrix \mathbf{H}_\perp shown in the edge labels. The direction of each edge is given by the sign of that element.

5.1.2. Random walk on the unipartite graph

In Davies et al. [2022], we showed that evidence flow has an interpretation in terms of a random walk. Consider a random walker moving on the unipartite NMA graph. The probability of the walker hopping from node v_j to node v_k at any time step is proportional to the weight w_{jk} of the direct estimate associated with that edge,

$$T_{jk} = \frac{w_{jk}}{\sum_{l \neq j} w_{jl}}. \quad (19)$$

If there is no direct comparison between the two treatments represented by these nodes, then no hop can occur. We set $T_{jj} = 0$ for all j and write \mathbf{T} for the transition matrix defined by these probabilities.

For a particular comparison of interest ab , node a is the initial state (source) of the walk and node b is the absorbing state (sink). The walker starts its journey at node a and hops around the network according to the transition probabilities in Equation (19) until it reaches node b . The random walk interpretation of the flow of evidence is then as follows:

Theorem 1 For the comparison of treatments a and b , the element of the aggregate hat matrix \mathbf{H}_\perp that defines the flow of evidence through the direct comparison jk is equal to the expected net number of times³ a random walker starting at node a on the unipartite NMA graph moves along the edge from v_j to v_k before it reaches node b .

In Davies et al. [2022] we proved this theorem using the pre-established analogies between (i) random walks and electrical networks (Doyle and Snell [1984]) and (ii) electrical networks and NMA (Rücker [2012]). We refer to the original article for details.

5.2. Bipartite evidence flow

The evidence flow network on the unipartite graph visualises how the direct evidence combines to give the network estimates. Papakonstantinou et al. [2018] showed that these flows can be used to calculate the proportion contributions of different paths of evidence. However, it is not clear how this relates to the contributions of individual trials. In this section, we instead use the arm-level hat matrix to construct an evidence flow network on the *bipartite* NMA graph.

³ The net number of times the walker moves from v_j to v_k is the number of crossings in the direction from v_j to v_k minus the number of crossings in the opposite direction.

5.2.1. The arm level hat matrix

The arm-level hat matrix $\mathbf{H}_{\top\perp}$ contains the coefficients of a linear equation relating the treatment effect estimates to the observations in each arm of each trial. Each column ij of $\mathbf{H}_{\top\perp}$ corresponds to an edge connecting trial node u_i to treatment node v_j in the bipartite graph. Each row kl corresponds to a comparison between two treatments, represented by bottom nodes v_k and v_l .

Similar to the aggregate hat matrix, the elements of each row of $\mathbf{H}_{\top\perp}$ have the properties of a flow network. We write $H_{\top\perp,ij}^{(kl)}$ for the element in row kl and column ij . We keep to our convention that i labels trials (top nodes) while indices j, k, l label treatments (bottom nodes). For a particular comparison kl , the arm-level hat matrix elements have the following properties:

1. the sum of outflows from node v_k is equal to one, $\sum_i H_{\top\perp,ki}^{(kl)} = 1$,
2. the sum of inflows to node v_l is equal to one, $\sum_i H_{\top\perp,il}^{(kl)} = 1$,
3. and at every intermediate node, the sum of outflows equals the sum of inflows. This is true for treatment nodes $v_j \neq v_k, v_l$,

$$\sum_i H_{\top\perp,ji}^{(kl)} = \sum_i H_{\top\perp,ij}^{(kl)}$$

and all trial nodes $u_i \in V_{\top}$,

$$\sum_j H_{\top\perp,ij}^{(kl)} = \sum_j H_{\top\perp,ji}^{(kl)}$$

Therefore, each row kl of $\mathbf{H}_{\top\perp}$ describes a directed network of flows on the bipartite graph that starts at node v_k and ends at node v_l . Due to the bipartite structure, edges are directed either from treatment nodes to trial nodes or vice versa. There can be no flow between two treatment nodes or between two trial nodes. The magnitude of flow between trial node u_i and treatment node v_j is given by the magnitude of the arm-level hat matrix coefficient $H_{\top\perp,ij}^{(kl)}$ associated with the observation in arm $t_{i,\ell} = j$ of trial i . The direction of flow is indicated by its sign.

The weight associated with each arm-level observation $\mu_{i,j}$ is given by the inverse of its variance. For the CE model this is $\sigma_{i,j}^{-2}$ and for the RE model, $(\sigma_{i,j}^2 + \frac{\tau^2}{2})^{-1}$. These are the weights associated with each edge in the bipartite graph. Panel (A) of Figure 4 shows the weighted bipartite graph for the fictional example in Table 3. The graph has $K_{\top\perp} = 12$ edges connecting each trial to the treatments it compares, $E_{\top\perp} = [1a, 1b, 2a, 2b, 2c, 3a, 3d, 4b, 4c, 4d, 5c, 5d]$. The thickness of each edge is proportional to the CE weight of that trial arm calculated from the inverse

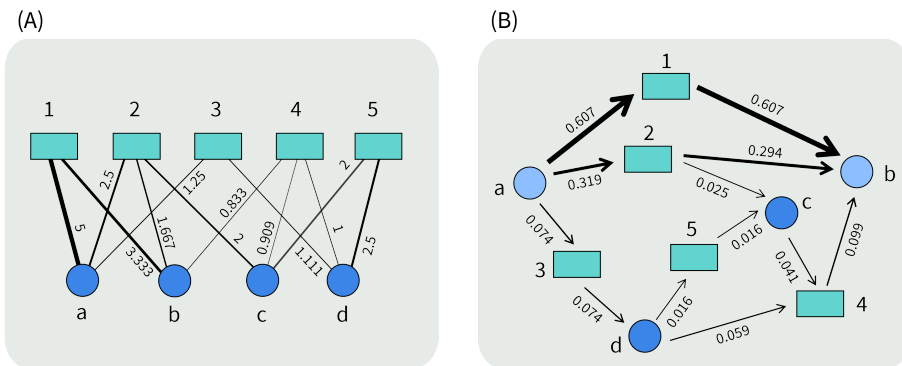


Fig. 4: (A) Weighted bipartite graph for the fictional example network described in Table 3. Rectangular nodes represent trials and circular nodes represent treatments. Each edge represents an arm of a trial. The thickness of an edge $[u_i, v_j]$ is proportional to the CE inverse-variance weight associated with that arm, $\sigma_{i,j}^{-2}$. These weights are shown in the edge labels. (B) The bipartite evidence flow network for the comparison of treatments a and b . The thickness of each edge is proportional to the corresponding element of the arm-level hat matrix $\mathbf{H}_{\top\perp}$ shown in the edge labels. The direction of each edge is given by the sign of that element.

arm-level variances in Table 3. These weights are shown in the edge labels. The corresponding weight matrix $W = \Sigma^{-1}$ is defined on the contrast-level and is given by

$$W = \begin{pmatrix} 2.000 & 0 & 0 & 0 & 0 & 0 & 0 \\ 0 & 1.216 & -0.541 & 0 & 0 & 0 & 0 \\ 0 & -0.541 & 1.351 & 0 & 0 & 0 & 0 \\ 0 & 0 & 0 & 0.588 & 0 & 0 & 0 \\ 0 & 0 & 0 & 0 & 0.608 & -0.331 & 0 \\ 0 & 0 & 0 & 0 & -0.331 & 0.635 & 0 \\ 0 & 0 & 0 & 0 & 0 & 0 & 1.111 \end{pmatrix}, \quad (20)$$

where each row and column represents a comparison to the trial-specific baseline in each trial. The design matrix of the network is

$$X = \begin{pmatrix} 1 & 0 & 0 \\ 1 & 0 & 0 \\ 0 & 1 & 0 \\ 0 & 0 & 1 \\ -1 & 1 & 0 \\ -1 & 0 & 1 \\ 0 & -1 & 1 \end{pmatrix}, \quad (21)$$

and the matrix relating the arm-level and contrast-level observations is

$$C = \begin{pmatrix} -1 & 1 & 0 & 0 & 0 & 0 & 0 & 0 & 0 & 0 & 0 & 0 \\ 0 & 0 & -1 & 1 & 0 & 0 & 0 & 0 & 0 & 0 & 0 & 0 \\ 0 & 0 & -1 & 0 & 1 & 0 & 0 & 0 & 0 & 0 & 0 & 0 \\ 0 & 0 & 0 & 0 & 0 & -1 & 1 & 0 & 0 & 0 & 0 & 0 \\ 0 & 0 & 0 & 0 & 0 & 0 & 0 & -1 & 1 & 0 & 0 & 0 \\ 0 & 0 & 0 & 0 & 0 & 0 & 0 & -1 & 0 & 1 & 0 & 0 \\ 0 & 0 & 0 & 0 & 0 & 0 & 0 & 0 & 0 & 0 & -1 & 1 \end{pmatrix}. \quad (22)$$

Substituting these matrices into Equation (9) yields the arm-level hat matrix,

$$H_{T\perp} = \begin{pmatrix} -0.607 & 0.607 & -0.319 & 0.294 & 0.025 & -0.074 & 0.074 & 0.099 & -0.041 & -0.059 & 0.016 & -0.016 \\ -0.280 & 0.280 & -0.519 & -0.113 & 0.632 & -0.201 & 0.201 & -0.167 & 0.166 & 0.001 & 0.202 & -0.202 \\ -0.252 & 0.252 & -0.362 & -0.031 & 0.394 & -0.386 & 0.386 & -0.221 & -0.045 & 0.265 & -0.349 & 0.349 \end{pmatrix},$$

where each column corresponds to an edge $\in E_{T\perp}$ and each row represents a comparison to the baseline; ab , ac , and ad .

The first row of $H_{T\perp}$ corresponds to comparison ab and describes a flow network on the bipartite graph from bottom node a to bottom node b . This is shown in panel (B) of Figure 4. The thickness of each edge is proportional to the magnitude of the associated coefficient and the direction is given by its sign. Unlike the unipartite flow network in Figure 3 (B), the bipartite representation shows how the evidence flows through the individual trials. For example, we see that the direct evidence comes from trials 1 and 2 with trial 1 exerting the most influence. The flow through the other three trial nodes is weaker, indicating that they make a smaller contribution to this comparison.

5.2.2. Random walk on the bipartite graph

Inspired by Zeng et al. [2024]'s recent work on higher order random walk (HoRW) models, we construct a random walk on the bipartite NMA graph. To do so, we define a weighted version of the biadjacency matrix B . Now, each element B_{ij} indicates not only the presence of edge $[u_i, v_j]$, but also its (inverse-variance) weight. For the RE model,

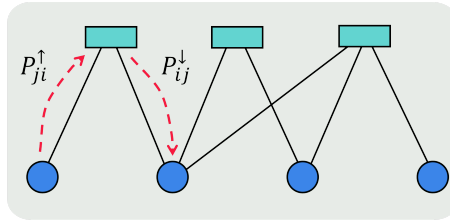


Fig. 5: An illustration of the higher order random walk (HoRW) on a bipartite graph. The walk consists of two parts: an upward walk from a bottom node v_j to a top node u_i with probability P_{ji}^{\uparrow} , and a downward walk from a top node u_i to a bottom node v_j with probability P_{ij}^{\downarrow} .

we have

$$B_{ij} = \begin{cases} (\sigma_{i,j}^2 + \frac{\tau^2}{2})^{-1} & \text{if } j \in \mathcal{T}_i \\ 0 & \text{otherwise,} \end{cases} \quad (23)$$

such that $B_{ij} > 0$ indicates that treatment j appears in trial i . For the CE model we set $\tau = 0$.

On the bipartite graph, a walker can only hop between top and bottom nodes. As shown in Figure 5, the HoRW is therefore made up of two parts: a downward walk from top to bottom, and an upward walk from bottom to top. We define the transition probabilities of these walks in terms of \mathbf{B} .

The downward walk involves a hop from a trial (top) node to a treatment (bottom) node. The transition probability of moving along an edge connecting two nodes is proportional to the weight associated with the corresponding trial arm. More specifically, the probability of hopping from trial node u_i to treatment node v_j at any time step is

$$P_{ij}^{\downarrow} = \frac{B_{ij}}{\sum_{j'=1}^N B_{ij'}}, \quad (24)$$

where the denominator is equal to the weighted degree of u_i , $\sum_{j'=1}^N B_{ij'} = \sum_{\ell=1}^{n_i} (\sigma_{i,t_{i\ell}}^2 + \frac{\tau^2}{2})^{-1}$. The $M \times N$ downstream transition matrix is then

$$\mathbf{P}^{\downarrow} = \mathbf{\Lambda}_{\top}^{-1} \mathbf{B}, \quad (25)$$

where $\mathbf{\Lambda}_{\top}$ is an $M \times M$ diagonal matrix whose diagonal elements are the weighted degrees of the trial nodes.

The upward walk is characterised by a hop from a treatment (bottom) node to a trial (top) node. As before, transition probabilities are proportional to the weights of the trial arms. This time, however, normalization is performed with respect to the weighted degree of the *treatment* node. The probability of hopping from treatment node v_j to trial node u_i is then

$$P_{ji}^{\uparrow} = \frac{B_{ij}}{\sum_{i'=1}^M B_{i'j}}, \quad (26)$$

where $\sum_{i'=1}^M B_{i'j} = \sum_{i' \in \mathcal{M}_j} (\sigma_{i',j}^2 + \frac{\tau^2}{2})^{-1}$ and $\mathcal{M}_j = [i' | \mathcal{T}_{i'} \supseteq j]$ is the set of trials containing treatment j . This yields the upstream transition matrix,

$$\mathbf{P}^{\uparrow} = \mathbf{\Lambda}_{\perp}^{-1} \mathbf{B}', \quad (27)$$

where $\mathbf{\Lambda}_{\perp}$ is an $N \times N$ diagonal matrix containing the weighted degrees of the treatment nodes.

The HoRW is fully described by the transition matrices \mathbf{P}^{\uparrow} and \mathbf{P}^{\downarrow} . As before, for a given treatment comparison ab , we define (bottom) node a as the initial state and (bottom) node b as the absorbing state. The walker starts at a

and hops between treatment and trial nodes according to P^\uparrow and P^\downarrow until it reaches b . Due to the bipartite structure, the walker cannot hop between two treatment nodes or between two trial nodes. Based on Theorem 1, we make the following conjecture relating this random walk to the bipartite evidence flow network:

Conjecture 1 *For the comparison of treatments a and b , the element of the arm-level hat matrix $\mathbf{H}_{\top\perp}$ that defines the flow of evidence through arm $t_{il} = j$ of trial i is equal to the expected net number of times a random walker starting at node a on the bipartite NMA graph moves along the edge from treatment node v_j to trial node u_i before it reaches node b .*

To prove this conjecture, we turn again to the analogies between NMA, electrical networks, and random walks described in Davies et al. [2022]. In Section D of the Supplementary Material, we extend these analogies to the bipartite framework and the HoRW. We summarize the main ideas below.

The weight of an edge in an electrical network is equal to the inverse of the resistance in that edge. Rücker [2012] showed that these resistances are analogous to variances in NMA. Therefore, we interpret the variance associated with each trial arm as a resistance in the corresponding edge of the bipartite graph. The resulting matrix of edge resistances, \mathbf{R} , has dimensions $K_{\top\perp} \times K_{\top\perp}$ and contains the arm-level variances, $\sigma_{i,j}^2 + \frac{\tau^2}{2}$, on its diagonal. It is related to the inverse-variance weight matrix via $\mathbf{W}^{-1} = \mathbf{C}\mathbf{R}\mathbf{C}'$. The analogy between electrical networks and random walks (Doyle and Snell [1984]) equates the movement of the random walker with the electrical current flowing through each edge in the network. In electrical network theory, the currents in each edge are calculated via

$$\mathbf{I}' = \mathbf{J}'(\mathbf{B}'_{\top\perp}\mathbf{R}^{-1}\mathbf{B}_{\top\perp})^+\mathbf{B}'_{\top\perp}\mathbf{R}^{-1}, \quad (28)$$

where $\mathbf{J}' = [\mathbf{0}_{(N-1) \times M} \ \mathbf{C}_N]$ is a matrix containing the currents at each node, $\mathbf{0}_{(N-1) \times M}$ is an $(N-1) \times M$ matrix of zeroes, and $\mathbf{B}_{\top\perp}$ is the oriented edge-vertex incidence matrix of the bipartite graph described in Section 4.3. To prove Conjecture 1, it suffices to show that \mathbf{I}' is equal to the arm-level hat matrix $\mathbf{H}_{\top\perp}$. We evaluate this conjecture empirically in Sections 6 and 7.

5.3. Unipartite flow from the bipartite random walk

As a final step, we use the random walk on the *bipartite* graph to obtain the original evidence flows on the *unipartite* graph. Following Zeng et al. [2024], we define a two-step random walk with an $N \times N$ transition matrix calculated from the upstream and downstream transition matrices,

$$\mathbf{P} = \mathbf{P}^\uparrow \mathbf{P}^\downarrow. \quad (29)$$

Each element P_{jk} describes the probability of two consecutive hops on the bipartite graph: a walker currently at bottom node v_j hops to any top node in the first step, followed immediately by a hop to bottom node v_k in the second step. The combination of these two consecutive steps defines a single transition (from node v_j to node v_k) on the unipartite projection of the bipartite graph. Therefore, for any treatment node v_j connected to a trial node u_i , there is always a non-zero probability for the walker to hop from v_j to u_i and then back to v_j in a single transition. This means $P_{jj} > 0$ for all j . In other words, the unipartite walk defined by \mathbf{P} allows the walker to remain at the same node at a given time step.

Given the random walk interpretation of evidence flow, we propose that the unipartite evidence flows described by the aggregate hat matrix \mathbf{H}_\perp can be obtained from the bipartite random walk as follows:

Conjecture 2 *For the comparison of treatments a and b , the element of the aggregate hat matrix \mathbf{H}_\perp that defines the flow of evidence through the direct comparison jk on the unipartite graph is equal to the expected net number of times a random walker starting at node a on the bipartite graph moves from (bottom node) v_j to (bottom node) v_k in two consecutive steps (via any trial node) before it reaches node b .*

In this conjecture, we are interested in the net number of times a walker moves along each edge as it travels from a to b . Any transitions that involve staying at a node do not affect these counts. We can adapt the two-step transition matrix \mathbf{P} to prohibit transitions to the same node; first setting the diagonal elements equal to zero, then renormalising the remaining probabilities in each row. We call the resulting matrix $\hat{\mathbf{P}}$. This matrix describes a

random walk on the unipartite graph that does not allow transitions to the same node ($\tilde{P}_{jj} = 0$) but yields the same expected number of edge crossings as the two-step walk described by P . In Theorem 1, we expressed the evidence flow in H_{\perp} in terms of a random walker moving on the unipartite graph according to the transition matrix T in Equation (19). By specifying $T_{jj} = 0$, this walk prohibits transitions to the same node. Therefore, to prove Conjecture 2 it suffices to show that the renormalised two-step transition matrix is equal to the unipartite matrix, $\tilde{P} = T$. We evaluate this conjecture empirically in the following sections.

6. Application to motivating data set

As an illustration, we return to the plaque psoriasis dataset described in Section 2. The treatments and trials define two sets of nodes,

$$(v_1, \dots, v_7) = (\text{ETN}, \text{IXE_Q2W}, \text{IXE_Q4W}, \text{PBO}, \text{SEC_150}, \text{SEC_300}, \text{UST}), \quad (30)$$

$$(u_1, \dots, u_9) = (\text{CLEAR}, \text{ERASURE}, \text{FEATURE}, \text{FIXTURE}, \text{IXORA-S}, \text{JUNCTURE}, \text{UNCOVER-1}, \text{UNCOVER-2}, \text{UNCOVER-3}). \quad (31)$$

We focus on the primary comparison of interest between v_2 : IXE_Q2W and v_6 : SEC_300, and explore the flow of evidence between these nodes on both the unipartite and bipartite graphs. In fitting the models, we choose common effects ($\tau = 0$) and use etanercept (v_1 : ETN) as the baseline treatment.

6.1. Unipartite evidence flow

6.1.1. The aggregate hat matrix

We begin by applying the aggregate model to explore evidence flow on the unipartite graph. The aggregate hat matrix H_{\perp} for the psoriasis dataset is shown in Appendix E, along with its component matrices B_{\perp} and W_{\perp} . Each row of H_{\perp} represents a comparison with the baseline, and each column represents an edge in the unipartite graph in Figure 2 (A). Columns are ordered according to the standard convention

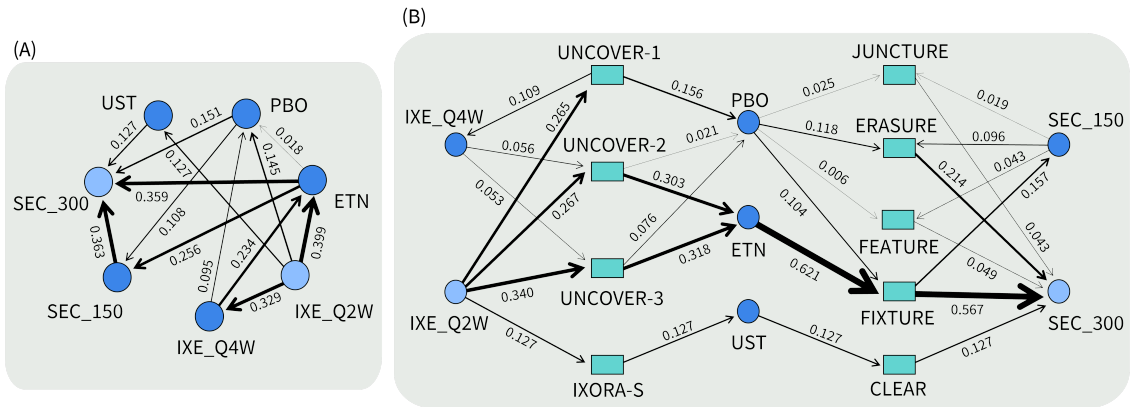


Fig. 6: (A) A unipartite evidence flow network for the plaque psoriasis NMA. In this example, the comparison of interest is between secukinumab 300mg (SEC_300) and ixekizumab every 2 weeks (IXE_Q2W). Evidence flows from node IXE_Q2W (the source) to node SEC_300 (the sink) along edges representing direct comparisons between treatments. The thickness of each edge is proportional to the corresponding element of the aggregate hat matrix H_{\perp} shown in the edge labels. The direction of each edge is given by the sign of that element. (B) The bipartite evidence flow network for the same comparison. Again, node IXE_Q2W is the source and node SEC_300 is the sink but now edges represent the arms of the trials. The thickness and direction of each edge is given by the magnitude and sign of the corresponding element of the arm-level hat matrix $H_{T\perp}$.

$([v_1, v_2], [v_1, v_3], \dots, [v_1, v_N], [v_2, v_3], [v_2, v_4], \dots, [v_2, v_N], \dots, [v_{N-1}, v_N])$. If there is no direct evidence on the comparison of treatments j and k , then there is no edge $[v_j, v_k]$ and that column is missing from H_\perp .

Since the comparison of interest (IXE_Q2W vs SEC_300) does not involve the baseline treatment (ETN), we calculate the relevant hat matrix elements using the consistency relations in Equation (7). Subtracting the row corresponding to the comparison of IXE_Q2W with the baseline from the row corresponding to the comparison of SEC_300 with the baseline gives

$$\begin{aligned} H_{\perp}^{(\text{IXE_Q2W, SEC_300})} &= H_{\perp}^{(\text{ETN, SEC_300})} - H_{\perp}^{(\text{ETN, IXE_Q2W})} \\ &= (-0.399, -0.234, 0.018, 0.256, 0.359, 0.329, 0.145, 0.127, 0.095, 0.108, 0.151, 0.363, -0.127). \end{aligned}$$

As shown in panel (A) of Figure 6, these values define an evidence flow network on the unipartite graph with a source at node IXE_Q2W and a sink at node SEC_300. The absence of an edge between these two nodes indicates that no trials have directly compared these treatments. Instead, most of the evidence on this comparison comes indirectly via node ETN. Looking at the original unipartite graph in Figure 2 (A), we might have expected that comparisons to placebo (PBO) would have a greater influence, since there are more trials involving this node. To explore this more thoroughly, we need to inspect the influence of individual trials and their arms.

6.1.2. Random walk on the unipartite graph

Using the aggregate weight matrix W_\perp , we define a random walk on the unipartite graph in Figure 2 (A). The transition matrix of this walk, calculated via Equation (19), is

$$T = \begin{pmatrix} 0 & 0.208 & 0.363 & 0.110 & 0.178 & 0.141 & 0 \\ 0.363 & 0 & 0.451 & 0.122 & 0 & 0 & 0.064 \\ 0.491 & 0.351 & 0 & 0.158 & 0 & 0 & 0 \\ 0.248 & 0.157 & 0.262 & 0 & 0.191 & 0.142 & 0 \\ 0.303 & 0 & 0 & 0.144 & 0 & 0.553 & 0 \\ 0.214 & 0 & 0 & 0.097 & 0.496 & 0 & 0.194 \\ 0 & 0.224 & 0 & 0 & 0 & 0.776 & 0 \end{pmatrix}, \quad (32)$$

where both rows and columns represent treatment nodes. Each element T_{jk} describes the probability of a walker currently at node v_j , hopping to node v_k in the next step. For example, the third row of T describes the transition probabilities for a walker at node v_3 : IXE_Q4W. From here, the walker can hop to adjacent nodes; v_1 : ETN with probability 0.491, v_2 : IXE_Q2W with probability 0.351, and v_4 : PBO with probability 0.158. The probability of hopping to any other node (not connected to IXE_Q4W) is zero. As required, these probabilities sum to one.⁴

6.2. Bipartite evidence flow

6.2.1. Arm-level hat matrix

Next, we apply the arm-level model to the psoriasis dataset and, for the same comparison of interest, explore the evidence flow on the bipartite graph. The arm-level hat matrix $H_{\top\perp}$ for the psoriasis dataset is shown in Section E of the Supplement along with the trial-level hat matrix H and their component matrices X , C , and Σ ($= W^{-1}$). Each row of $H_{\top\perp}$ corresponds to a comparison with the baseline treatment and each column represents an edge in the bipartite graph (Figure 2 (B)). These columns are ordered according to the convention $([u_1, v_2], \dots, [u_1, v_N], [u_2, v_1], \dots, [u_2, v_N], \dots, [u_M, v_1], \dots, [u_M, v_N])$. If trial i does not involve treatment j , then there is no edge $[u_i, v_j]$ and this column does not appear in $H_{\top\perp}$.

As above, we obtain the hat matrix elements for the comparison of interest by applying the consistency equations,

$$\begin{aligned} H_{\top\perp}^{(\text{IXE_Q2W, SEC_300})} &= H_{\top\perp}^{(\text{ETN, SEC_300})} - H_{\top\perp}^{(\text{ETN, IXE_Q2W})} \\ &= (0.127, -0.127, -0.118, -0.096, 0.214, -0.006, -0.043, 0.049, -0.621, -0.104, 0.157, 0.567, -0.127, 0.127, \\ &\quad -0.025, -0.019, 0.043, -0.265, 0.109, 0.156, 0.303, -0.267, -0.056, 0.021, 0.318, -0.340, -0.053, 0.076). \end{aligned}$$

⁴ NB: All rows of the transition matrices sum to exactly one, although this may not always appear to be the case due to rounding.

Panel (B) in Figure 6 shows the corresponding evidence flow network from IXE_Q2W to SEC_300 on the bipartite graph. As before, we observe that this comparison relies strongly on indirect evidence via treatment ETN. More specifically, we now also observe that this indirect evidence arises primarily from the UNCOVER-2, UNCOVER-3 and FIXTURE trials. Each of these trials also involves a comparison to placebo, but the evidence flow is much smaller through these arms compared with the active intervention arms. On inspection of the data, we discover that placebo arms have lower event rates which causes them to have lower precision and therefore, less influence.

6.2.2. Random walk on the bipartite graph

Next, we define transition probabilities for the random walk on the bipartite graph in Figure 2 (B). Each edge represents the arm of a trial and is weighted by the inverse of the variance associated with the observation in that arm. We use these weights to construct the weighted biadjacency matrix \mathbf{B} shown in Appendix E. Via Equation (24), we then obtain the transition matrix of the downward walk,

$$\mathbf{P}^\downarrow = \begin{pmatrix} 0 & 0 & 0 & 0 & 0 & 0.330 & 0.670 \\ 0 & 0 & 0 & 0.113 & 0.509 & 0.378 & 0 \\ 0 & 0 & 0 & 0.020 & 0.517 & 0.462 & 0 \\ 0.355 & 0 & 0 & 0.070 & 0.322 & 0.254 & 0 \\ 0 & 0.197 & 0 & 0 & 0 & 0 & 0.803 \\ 0 & 0 & 0 & 0.111 & 0.567 & 0.322 & 0 \\ 0 & 0.300 & 0.527 & 0.172 & 0 & 0 & 0 \\ 0.481 & 0.154 & 0.340 & 0.025 & 0 & 0 & 0 \\ 0.491 & 0.178 & 0.244 & 0.087 & 0 & 0 & 0 \end{pmatrix}, \quad (33)$$

where rows represent trials and columns represent treatments. Each element P_{ij}^\downarrow describes the probability of a walker currently at trial node u_i , hopping to treatment node v_j in the next step. For example, the first row contains the transition probabilities for a walker at trial node u_1 : CLEAR. This trial has two arms, and the walker can hop to either one of these treatments in the next step; v_6 : SEC_300 with probability 0.330, or v_7 : UST with probability 0.670. The probability of hopping to another trial node, or to a treatment that does not appear in that trial is zero.

Similarly, we obtain the upstream transition matrix via Equation (26),

$$\mathbf{P}^\uparrow = \begin{pmatrix} 0 & 0 & 0 & 0.307 & 0 & 0 & 0 & 0.329 & 0.364 \\ 0 & 0 & 0 & 0 & 0.062 & 0 & 0.352 & 0.260 & 0.325 \\ 0 & 0 & 0 & 0 & 0 & 0 & 0.377 & 0.350 & 0.273 \\ 0 & 0.152 & 0.007 & 0.218 & 0 & 0.033 & 0.296 & 0.061 & 0.233 \\ 0 & 0.337 & 0.086 & 0.494 & 0 & 0.083 & 0 & 0 & 0 \\ 0.196 & 0.264 & 0.081 & 0.410 & 0 & 0.050 & 0 & 0 & 0 \\ 0.673 & 0 & 0 & 0 & 0.327 & 0 & 0 & 0 & 0 \end{pmatrix}. \quad (34)$$

Here, rows represent treatments and columns represent trials, such that an element P_{ji}^\uparrow describes the probability of a walker currently at bottom node v_j , hopping to top node u_i in the next step. Similar to matrix \mathbf{T} in Equation (32), the third row of \mathbf{P}^\uparrow contains the transition probabilities for a walker at treatment node v_3 : IXE_Q4W. However, rather than hopping to another treatment node, this walker can only hop to the trials (top nodes) in which it appears; u_7 : UNCOVER-1 with probability 0.377, u_8 : UNCOVER-2 with probability 0.350 and u_9 : UNCOVER-3 with probability 0.273. The probability of hopping to another treatment node, or to a trial that does not contain IXE_Q4W is zero.

6.3. Conjectures

Finally, we use our results for the psoriasis dataset to check whether our two conjectures hold.

6.3.1. Conjecture 1

To check Conjecture 1, we compare the arm-level hat matrix $\mathbf{H}_{\top\perp}$ with the matrix of nodal currents \mathbf{I}' calculated via Equation (28). In Section E of the Supplementary Material we show \mathbf{I}' for the psoriasis data along with its

component matrices J' , $B_{T\perp}$, and R . Comparing each element of I' with the corresponding element of $H_{T\perp}$ gives a maximum absolute difference of 2.44×10^{-15} . As a general rule of thumb, two values can be considered numerically identical if their absolute difference is less than the square root of the machine precision (Higham [2002]). For the machine used in these calculations, this value was 1.49×10^{-8} . Therefore, for the psoriasis dataset, these two matrices are numerically identical, supporting Conjecture 1.

6.3.2. Conjecture 2

To check Conjecture 2, we calculate the two-step transition matrix P via Equation (29) using the upstream and downstream transition matrices in Equations (33) and (34). Each element P_{jk} of this matrix describes the probability that a walker currently at bottom node v_j on the bipartite graph hops to bottom node v_k in the next two consecutive steps (via any top node). The renormalised transition matrix \tilde{P} is obtained by setting the diagonal elements of P equal to zero and renormalising the remaining probabilities in each row. In Section E of the Supplement we show both P and \tilde{P} for the psoriasis dataset. Comparing each element of \tilde{P} with the corresponding element of T in Equation (32) gives a maximum absolute difference of 1.33×10^{-15} . Therefore, these two matrices can be considered numerically identical, meaning Conjecture 2 holds for this dataset.

7. Simulations

In Section 6 we showed that Conjectures 1 and 2 hold true for the psoriasis dataset. To investigate this more thoroughly, we evaluate the two conjectures for 10,000 randomly generated NMA graphs. We describe our simulation method in Section F of the Supplementary Material. This involves generating random network structures (i.e. which treatments appear in which trials) as well as sampling the outcome data in each trial. As shown in the Supplement, the bipartite representation of NMA provides a natural framework for automatically generating networks with multi-arm trials.

For each randomly generated NMA, we evaluate Conjecture 1 by comparing each element of $H_{T\perp}$ with the corresponding element of I' . Across all 10,000 networks, the maximum difference between two equivalent elements was 6.03×10^{-11} . Similarly, to evaluate Conjecture 2 we compare T and \tilde{P} for each network. Here, the maximum difference between two corresponding elements was 1.15×10^{-13} . This provides strong empirical evidence for both conjectures.

8. Summary and discussion

In this paper, we have formalised the bipartite framework for NMA. Treatments and trials define two distinct types of node, while edges correspond to the arms of a trial, connecting each trial node to the treatments it compares. This representation accurately describes the data structure of NMA, showing which treatments have been compared in which trials. Unlike the traditional representation of NMA as a unipartite graph, the bipartite graph shows comparisons from trials that compare more than two treatments.

Understanding how evidence from different trials combines to give overall estimates of treatment effects is a key challenge for NMA. The influence of observations from the different trials is related to the structure of the network and the weight assigned to each observation in the model. This information is captured in the model's hat matrix. In earlier work, König et al. [2013] used the hat matrix of the aggregate model to define an evidence flow network on the unipartite NMA graph. However, it is not clear how these flows relate to the contributions of individual trials. Our work overcomes this limitation by instead characterizing the evidence flow on the bipartite graph. We considered an 'arm level' parameterization of the standard NMA model that expresses the treatment effect estimates as a linear combination of the observations in each arm of each trial. By linking this model to the bipartite framework, we showed that the elements in each row of the arm-level hat matrix define the evidence flow through each edge in the bipartite graph. This approach reveals how evidence flows through the individual trials.

In practice, arm-level observations will not always be available. Instead, trials might report relative effects with respect to some reference arm. However, to construct the arm-level hat matrix we only need the variances associated with the observations. In fact, the arm-level hat matrix is just a projection of the standard trial-level hat matrix which depends on the variances and covariances of the contrast-level observations. The covariance between contrast-level observations in a trial is the variance in the reference arm of that trial. If this information is not

available, it can be approximated (see e.g. Dias et al. [2011], Riley [2009]). Assuming arms are independent, the arm-level variances can be reconstructed from the contrast-level variances and the variance in the reference arm. Therefore, the arm-level hat matrix requires no additional information compared with the standard model.

Using the analogy between random walks and evidence flow set out in Davies et al. [2022], we defined a higher order random walk on the bipartite graph. The walk is made up of two parts: ‘upward’ transitions from treatments to trials, and ‘downward’ transitions from trials to treatments. Previously, Davies et al. [2022] showed that the movement of a random walker on the NMA graph contains information about the propagation of evidence through the network. Therefore, we proposed a conjecture linking the HoRW to the bipartite evidence flow network. This provides a random walk interpretation for the flow of evidence through the arms of the trials. We then proposed a second conjecture, describing how the original evidence flows on the unipartite graph can be derived from the HoRW. This result reveals the connection between the evidence structures in the unipartite and bipartite frameworks. We verified both conjectures in an application to a real dataset and in extensive simulations on randomly generated graphs. However, theoretical proofs of these conjectures remain an open challenge.

One limitation of the bipartite framework as a visualization of NMA is that these graphs quickly become large and complex as the number of treatments and trials increases. For larger networks, it is increasingly difficult to arrange the bipartite graph in a way that clearly shows the flow of evidence between two treatments. This points to a need for more sophisticated visualization tools developed specifically for this framework. We note, however, that the utility of the bipartite framework for NMA is not only related to visualization. The bipartite graph is an accurate mathematical description of the data structure. By setting out this framework, NMA can access the suite of tools and techniques developed for the study of bipartite structures in other areas of network science.

Indeed, the bipartite framework for NMA opens up many avenues for future applications and developments. A natural next step of the work we have described is to use the flow of information in the bipartite graph to evaluate the influence of trials. This is the subject of ongoing research that we expect will overcome the limitations of previous attempts at this task (e.g. Lu et al. [2011], Krahn et al. [2013], Jackson et al. [2017], Riley et al. [2018], Copas et al. [2018], Papakonstantinou et al. [2018], Rücker et al. [2020]). We also predict that the random walk interpretation of evidence flow will provide a numerical tool to uncover the contribution of trials in more complex multi-parameter evidence synthesis models. In our simulations, we made use of a simple bipartite random graph model to generate synthetic networks with multi-arm trials. In another parallel project, we are further developing this algorithm to produce networks with more realistic characteristics. Related to this, previous work has attempted to characterize the structure (or geometry) of NMA networks (e.g. Salanti et al. [2008], Nikolakopoulou et al. [2014], Tonin et al. [2019], Papakonstantinou et al. [2020]). Using the bipartite description of NMA, we can more accurately evaluate the properties of these data structures. It will then be interesting to investigate how features of the bipartite graph are related to the performance of the NMA. Finally, Lumley [2024] proposed the bipartite representation of NMA as a tool to identify inconsistencies between different sources of evidence in the network. He predicted that this would alleviate the challenges faced when loops of evidence involve estimates from multi-arm trials.

This work marks the first application of higher-order network theory in the context of NMA. The bipartite framework provides new insights into the evidence structure and the role of individual trials in NMA estimates. It also lays the groundwork for future methodological advancements and applications. The study of higher order interactions is a young and actively evolving research area in network science. By framing NMA in this context, we have enabled access to state of the art techniques developed in this area. Moreover, there is now an exciting opportunity for NMA to shape the direction of research in this emerging field.

Acknowledgments

ALD acknowledges funding from the Engineering and Physical Sciences Research Council (EP/Y007905/1). I would like to thank my fellowship advisory group for their valuable insights and feedback throughout the progression of this paper: Gerta Rücker, Ian White, Nicky Welton, Julian Higgins, Ayavaldi Ganesh, and Guido Schwarzer. I also thank David Phillippo for many useful discussions particularly regarding notation and presentation.

References

- A. C. Aitken. Iv.—on least squares and linear combination of observations. *Proceedings of the Royal Society of Edinburgh*, 55:42–48, 1936. doi: 10.1017/S0370164600014346.
- R. Albert, H. Jeongand, and A. Barabási. Error and attack tolerance of complex networks. *Nature*, 406:378–382, 2000. doi: 10.1038/35019019.
- A. Barabasi and R. Albert. Emergence of scaling in random networks. *Science*, 286(5439):509–512, 1999.
- P. Bonacich. Power and centrality: a family of measures. *Am. J. Sociol.*, 92:1170–1182, 1987.
- J. B. Copas, D. Jackson, I. R. White, and R. D. Riley. The Role of Secondary Outcomes in Multivariate Meta-Analysis. *Journal of the Royal Statistical Society Series C: Applied Statistics*, 67(5):1177–1205, 03 2018. ISSN 0035-9254. doi: 10.1111/rssc.12274.
- G. Csardi and T. Nepusz. The igraph software package for complex network research. *InterJournal*, Complex Systems:1695, 2006. URL <https://igraph.org>.
- G. Csárdi, T. Nepusz, V. Traag, S. Horvát, F. Zanini, D. Noom, and K. Müller. *igraph: Network Analysis and Visualization in R*, 2025. URL <https://CRAN.R-project.org/package=igraph>. R package version 2.1.4.
- A. L. Davies and T. Galla. Network meta-analysis: a statistical physics perspective. *Journal of Statistical Mechanics: Theory and Experiment*, 2022(11):11R001, 2022. doi: 10.1088/1742-5468/ac9463.
- A. L. Davies, T. Papakonstantinou, A. Nikolakopoulou, G. Rücker, and T. Galla. Network meta-analysis and random walks. *Statistics in Medicine*, 41(12):2091–2114, 2022. doi: <https://doi.org/10.1002/sim.9346>.
- S. Dias, N. J. Welton, A. J. Sutton, and A. E. Ades. NICE DSU technical support document 2: A generalised linear modelling framework for pairwise and network meta-analysis of randomised controlled trials. Technical report, National Institute for Health and Care Excellence, Decision Support Unit, 2011. URL <http://www.nicedsu.org.uk/>.
- S. Dias, A. E. Ades, N. J. Welton, J. P. Jansen, and A. J. Sutton. *Network Meta-Analysis for Decision Making*. Wiley, Oxford, UK, 2018.
- P. Doyle and J. Snell. *Random Walks and Electric Networks*. The Carus Mathematical Monographs. The American Mathematical Society, Washington D. C., 1984. doi: <https://doi.org/10.5948/upo9781614440222>.
- P. Erdos and A. Renyi. On random graphs I. *Publ. Math.*, Debrecen 6:290–297, 1959.
- P. Erdos and A. Renyi. On the evolution of random graphs. *Publication of the Mathematical Institute of the Hungarian Academy of Sciences*, pages 17–61, 1960.
- M. T. Gastner and M. E. J. Newman. The spatial structure of networks. *The European Physical Journal B - Condensed Matter and Complex Systems*, 49:247–252, 2006. doi: 10.1140/epjb/e2006-00046-8.
- C. Godsil and G. Royle. *The Laplacian of a Graph*, pages 279–306. Springer New York, New York, NY, 2001. ISBN 978-1-4613-0163-9. doi: 10.1007/978-1-4613-0163-9_13.
- J. Guillaume and M. Latapy. Bipartite structure of all complex networks. *Inf. Process. Lett.*, 90(5):215–221, 2004.
- J.-L. Guillaume and M. Latapy. Bipartite graphs as models of complex networks. *Physica A: Statistical Mechanics and its Applications*, 371(2):795–813, 2006. ISSN 0378-4371. doi: <https://doi.org/10.1016/j.physa.2006.04.047>.
- I. Gutman and W. Xiao. Generalized inverse of the Laplacian matrix and some applications. *Bulletin T.CXXIX de l'Académie serbe des sciences et des arts*, 29:15–23, 2004.
- J. P. T. Higgins and A. Whitehead. Borrowing strength from external trials in a meta-analysis. *Stat. Med.*, 15:2733–2749, 1996.
- N. J. Higham. *Accuracy and Stability of Numerical Algorithms*. Society for Industrial and Applied Mathematics, second edition, 2002. doi: 10.1137/1.9780898718027.
- D. Jackson, I. R. White, M. Price, J. Copas, and R. D. Riley. Borrowing of strength and study weights in multivariate and network meta-analysis. *Statistical Methods in Medical Research*, 26(6):2853–2868, 2017. doi: 10.1177/0962280215611702.
- S. Kanters, M. E. Karim, K. Thorlund, A. Anis, and N. Bansback. When does the use of individual patient data in network meta-analysis make a difference? a simulation study. *BMC Medical Research Methodology*, 21(21), 2021. doi: 10.1186/s12874-020-01198-2.
- U. Krahn, H. Binder, and J. König. A graphical tool for locating inconsistency in network meta-analyses. *BMC Med Res Methodol*, 13(35):1–18, 2013.
- A. Krause, K. Frank, D. Mason, R. Ulanowicz, and W. Taylor. Compartments revealed in food-web structure. *Nature*, 426:282–5, 12 2003. doi: 10.1038/nature02115.
- J. König, U. Krahn, and H. Binder. Visualizing the flow of evidence in network meta-analysis and characterizing mixed treatment comparisons. *Stat Med*, 32(30):5414–5429, 2013.
- D. Liben-Nowell and J. Kleinberg. Tracing information flow on a global scale using internet chain-letter data. *Proceedings of the National Academy of Sciences*, 105(12):4633–4638, 2008. doi: 10.1073/pnas.0708471105.
- G. Lu and A. E. Ades. Combination of direct and indirect evidence in mixed treatment comparisons. *Stat. Med.*, 23:3105–3124, 2004.
- G. Lu, N. J. Welton, J. Higgins, I. White, and A. Ades. Linear inference for mixed treatment comparison meta-analysis: a two-stage approach. *Res Synth Methods*, 2(1):43–60, 2011.
- T. Lumley. Network meta-analysis for indirect treatment comparisons. *Stat. Med.*, 21:2313–2324, 2002.
- T. Lumley. Network meta-analysis: Looping back. *Research Synthesis Methods*, n/a(n/a), 2024. doi: <https://doi.org/10.1002/jrsm.1743>.

- B. Mohar. Graph Laplacians. In L. W. Beineke, R. J. Wilson, and P. J. Cameron, editors, *Topics in Algebraic Graph Theory*, pages 113–136. Cambridge University Press, New York, NY, 2005. ISBN 0-521-80197-4.
- M. E. J. Newman. Scientific collaboration networks. I. network construction and fundamental results. *Phys. Rev. E*, 64:016131, Jun 2001a. doi: 10.1103/PhysRevE.64.016131.
- M. E. J. Newman. Scientific collaboration networks. II. shortest paths, weighted networks, and centrality. *Phys. Rev. E*, 64:016132, Jun 2001b. doi: 10.1103/PhysRevE.64.016132.
- A. Nikolakopoulou, A. Chaimani, A. A. Veroniki, H. S. Vasiliadis, C. H. Schmid, and G. Salanti. Characteristics of networks of interventions: A description of a database of 186 published networks. *PLOS ONE*, 9(1):1–10, 01 2014. doi: 10.1371/journal.pone.0086754.
- T. Papakonstantinou, A. Nikolakopoulou, G. Rücker, A. Chaimani, G. Schwarzer, M. Egger, and G. Salanti. Estimating the contribution of studies in network meta-analysis: paths, flows and streams. *F1000Research*, 7, 2018.
- T. Papakonstantinou, A. Nikolakopoulou, M. Egger, and G. Salanti. In network meta-analysis, most of the information comes from indirect evidence: empirical study. *Journal of Clinical Epidemiology*, 124:42–49, 2020. doi: 10.1016/j.jclinepi.2020.04.009.
- D. M. Phillippo. multinma: Bayesian network meta-analysis of individual and aggregate data. R package version 0.7.2, 2024.
- R. D. Riley. Multivariate meta-analysis: The effect of ignoring within-study correlation. *Journal of the Royal Statistical Society Series A: Statistics in Society*, 172(4):789–811, 04 2009. ISSN 0964-1998. doi: 10.1111/j.1467-985X.2008.00593.x.
- R. D. Riley, J. Ensor, D. Jackson, and D. L. Burke. Deriving percentage study weights in multi-parameter meta-analysis models: with application to meta-regression, network meta-analysis and one-stage individual participant data models. *Statistical Methods in Medical Research*, 27(10):2885–2905, 2018. doi: 10.1177/0962280216688033. PMID: 28162044.
- G. Rücker. Network meta-analysis, electrical networks and graph theory. *Res Synth Methods*, 3(4):312–324, 2012.
- G. Rücker and G. Schwarzer. Reduce dimension or reduce weights? comparing two approaches to multi-arm studies in network meta-analysis. *Stat Med*, 33(25):4353–4369, 2014.
- G. Rücker, A. Nikolakopoulou, T. Papakonstantinou, G. Salanti, R. D. Riley, and G. Schwarzer. The statistical importance of a study for a network meta-analysis estimate. *BMC Med Res Methodol*, 20(190), 2020. doi: <https://doi.org/10.1186/s12874-020-01075-y>.
- G. Rücker, T. Papakonstantinou, A. Nikolakopoulou, G. Schwarzer, T. Galla, and A. L. Davies. Shortest path or random walks? a framework for path weights in network meta-analysis. *Statistics in Medicine*, 43(22):4287–4304, 2024. doi: <https://doi.org/10.1002/sim.10177>.
- G. Salanti, F. K. Kavvoura, and J. P. Ioannidis. Exploring the geometry of treatment networks. *Annals of Internal Medicine*, 148(7):544–553, 2008. doi: 10.7326/0003-4819-148-7-200804010-00011. PMID: 18378949.
- P. Sen, S. Dasgupta, A. Chatterjee, P. A. Sreeram, G. Mukherjee, and S. S. Manna. Small-world properties of the Indian railway network. *Phys. Rev. E*, 67:036106, Mar 2003. doi: 10.1103/PhysRevE.67.036106.
- R. V. Solé et al. The small world of human language. *Proceedings. Biological Sciences*, 268(1482):2261–2265, 2001.
- O. Sporns. Network analysis, complexity, and brain function. *Complexity*, 8(1):56–60, 2002. doi: <https://doi.org/10.1002/cplx.10047>.
- J. Stoer and R. Bulirsch. *Introduction to Numerical Analysis*. Springer-Verlag, New York, 3 edition, 2002.
- F. S. Tonin, H. H. Borba, A. M. Mendes, A. Wiens, F. Fernandez-Llimos, and R. Pontarolo. Description of network meta-analysis geometry: A metrics design study. *PLOS ONE*, 14(2):1–14, 02 2019. doi: 10.1371/journal.pone.0212650.
- T. Walsh. Hypermaps versus bipartite maps. *Journal of Combinatorial Theory, Series B*, 18(2):155–163, 1975. ISSN 0095-8956. doi: [https://doi.org/10.1016/0095-8956\(75\)90042-8](https://doi.org/10.1016/0095-8956(75)90042-8).
- R. Warren, A. Brnabic, D. Saure, R. Langley, K. See, J. Wu, A. Schacht, L. Mallbris, and A. Nast. Matching-adjusted indirect comparison of efficacy in patients with moderate-to-severe plaque psoriasis treated with ixekizumab vs. secukinumab. *British Journal of Dermatology*, 178(5):1064–1071, 05 2018. ISSN 0007-0963. doi: 10.1111/bjd.16140.
- D. J. Watts and S. H. Strogatz. Collective dynamics of ‘small-world’ networks. *Nature*, 393(6684):440–442, 1998.
- I. R. White, R. M. Turner, A. Karahalios, and G. Salanti. A comparison of arm-based and contrast-based models for network meta-analysis. *Statistics in Medicine*, 38(27):5197–5213, 2019. doi: <https://doi.org/10.1002/sim.8360>.
- W. Zachary. An information flow model for conflict and fission in small groups. *Journal of anthropological research*, 33:452–473, 11 1976. doi: 10.1086/jar.33.4.3629752.
- Y. Zeng, Y. Huang, X.-L. Ren, and L. Lü. Identifying vital nodes through augmented random walks on higher-order networks. *Information Sciences*, 679:121067, 2024. ISSN 0020-0255. doi: <https://doi.org/10.1016/j.ins.2024.121067>.

Supplementary Material

A. Design matrix

The design matrix in the definition of the trial-level hat matrix (Equation (4) in the main text) describes which treatments are compared in each trial. Each trial contributes an $(n_i - 1) \times (N - 1)$ matrix X_i such that $X = [X_1 \ X_2 \ \dots \ X_M]'$. Each of the $N - 1$ columns of X_i represents a comparison between treatment $j = 2, \dots, N$ and the global baseline $j = 1$. The $n_i - 1$ rows represent the comparisons of treatments $[t_{i,\ell}; \ell = 2, \dots, n_i]$ to the trial-specific baseline $t_{i,1}$. A given row ℓ contains a +1 in the column corresponding to $j = t_{i,\ell}$. If the trial-specific baseline is not the global baseline ($t_{i,1} \neq 1$), then there is a -1 in the column corresponding to $j = t_{i,1}$. All other entries are zero.

B. Aggregate Model

In this section, we summarize the aggregate version of the graph theoretical model. For details of this model, and how it corresponds to other formulations we refer to Davies et al. [2022] and the Supplementary Materials therein.

Each n_i -armed trial is associated with $q_i = n_i(n_i - 1)/2$ contrast-level observations representing comparisons between each pair of treatments in the trial. For a trial with $n_i = 2$ arms, the weight of each observation is given by its inverse variance $w_{i,t_{i\ell}t_{i\ell'}} = (\sigma_{t_{i\ell}t_{i\ell'}}^2 + \tau^2)^{-1}$ (where $\tau = 0$ for a CE model and must be estimated in an RE model). For a trial with $n_i > 2$, we account for correlations by adjusting the variances using a method described in Rücker [2012], Rücker and Schwarzer [2014] and Gutman and Xiao [2004]. This results in a set of q_i adjusted weights $[w_{i,t_{i\ell}t_{i\ell'}}; \ell = 1, \dots, n_i - 1, \ell' = \ell + 1, \dots, n_i]$ describing a fully-connected subgraph of q_i 2-armed trials that is equivalent to the original multi-arm trial.

In step 1 of the aggregate model, we use the adjusted weights to perform a pairwise meta-analysis for each pair of treatments jk that have been compared in at least one trial (i.e. across each of the K_\perp edges in the unipartite graph). The resulting direct estimate of this comparison is a weighted mean

$$\hat{\theta}_{jk}^{\text{dir}} = \frac{\sum_{i \in \mathcal{M}_{jk}} w_{i,jk} y_{i,jk}}{\sum_{i \in \mathcal{M}_{jk}} w_{i,jk}}, \quad (\text{B.1})$$

where we have written \mathcal{M}_{jk} for the set of trials involving treatments j and k . That is, $\mathcal{M}_{jk} = [i | \mathcal{T}_i \supseteq [j, k]]$. The inverse variance of the direct estimate is then

$$w_{jk} = \sum_{i \in \mathcal{M}_{jk}} w_{i,jk}. \quad (\text{B.2})$$

We collect the direct estimates in a K_\perp -dimensional vector $\hat{\theta}^{\text{dir}}$ and the inverse-variances in a $K_\perp \times K_\perp$ diagonal matrix $\mathbf{W}_\perp = \text{diag}(w_{jk})$. The matrix \mathbf{W}_\perp then defines a set of edge weights, where each element w_{jk} is the weight associated with edge $[v_j, v_k]$ in the unipartite graph.

In the second step, we use the edge weights to combine the direct estimates in an NMA. To do so, we make use of the oriented edge-vertex incidence matrix of the unipartite graph \mathbf{B}_\perp described in Section 4.1 in the main paper. Without loss of generality, each row representing an edge $[v_j, v_k]$ is given an arbitrary orientation, with a -1 in column j and +1 in column k . The network estimates of the basic parameters are then obtained via

$$\hat{\theta} = \mathbf{H}_\perp \hat{\theta}^{\text{dir}}, \quad (\text{B.3})$$

where we write \mathbf{H}_\perp for the $(N - 1) \times K_\perp$ aggregate hat matrix, defined as

$$\mathbf{H}_\perp = \mathbf{C}_N (\mathbf{B}_\perp' \mathbf{W}_\perp \mathbf{B}_\perp)^+ \mathbf{B}_\perp' \mathbf{W}_\perp. \quad (\text{B.4})$$

The $N \times N$ matrix $\mathbf{L}_\perp = \mathbf{B}_\perp' \mathbf{W}_\perp \mathbf{B}_\perp$ is the Laplacian of the weighted unipartite graph and \mathbf{L}_\perp^+ denotes its Moore-Penrose pseudo-inverse (Gutman and Xiao [2004]). The Laplacian is a matrix representation of a graph, related to many of its key properties. For more information, we refer the interested reader to various sources e.g. Rücker

[2012], Gutman and Xiao [2004], Godsil and Royle [2001], and Mohar [2005]. Recall from the main paper (Section 3.1) the definition of matrix $C_N = [-\mathbf{1}_{N-1} \ \mathbf{I}_{N-1}]$. In Equation (B.4), this matrix ensures that H_\perp has the correct dimensions for projecting onto the $N - 1$ basic parameters. Similar to the trial-level hat matrix, each row of H_\perp contains the coefficients of a linear equation describing how the estimates of each basic parameter $\hat{\theta}_{1j}$ depend on the direct estimates associated with each edge in the unipartite graph, $\hat{\theta}_{jk}^{\text{dir}}; [v_j, v_k] \in E_\perp$. As before, we obtain the full version of the aggregate hat matrix by applying the consistency equations in Equation (7) in the main paper.

C. Edge vertex incidence matrix of the bipartite graph

Figure 1 (D) in the main paper shows the bipartite graph for an NMA of six treatments, $[a, b, c, d, e, f]$, compared in three trials, $u_1 = [b, c]$, $u_2 = [c, e, f]$, and $u_3 = [a, b, d, e]$. The corresponding edge-vertex incidence matrix of this graph is given by

$$B_{\top\perp} = \begin{matrix} & u_1 & u_2 & u_3 & a & b & c & d & e & f \\ \begin{matrix} [u_1, b] \\ [u_1, c] \\ [u_2, a] \\ [u_2, b] \\ [u_2, d] \\ [u_2, e] \\ [u_3, c] \\ [u_3, e] \\ [u_3, f] \end{matrix} & \begin{pmatrix} 1 & 0 & 0 & 0 & 1 & 0 & 0 & 0 & 0 \\ 1 & 0 & 0 & 0 & 0 & 1 & 0 & 0 & 0 \\ 0 & 1 & 0 & 1 & 0 & 0 & 0 & 0 & 0 \\ 0 & 1 & 0 & 0 & 1 & 0 & 0 & 0 & 0 \\ 0 & 1 & 0 & 0 & 0 & 0 & 1 & 0 & 0 \\ 0 & 1 & 0 & 0 & 0 & 0 & 0 & 1 & 0 \\ 0 & 0 & 1 & 0 & 0 & 1 & 0 & 0 & 0 \\ 0 & 0 & 1 & 0 & 0 & 0 & 0 & 1 & 0 \\ 0 & 0 & 1 & 0 & 0 & 0 & 0 & 0 & 1 \end{pmatrix} \end{matrix}, \quad (\text{C.5})$$

where each row represents an edge $\in E_{\top\perp}$ between a top and bottom node, and each column represents a node. The first M columns correspond to top nodes $\in V_\top$ and the last N columns correspond to bottom nodes $\in V_\perp$.

D. Electrical networks and bipartite NMA

D.1. Unipartite framework

D.1.1. NMA and electrical networks

In an electrical network, edges represent resistors that connect at the nodes. If two (or more) nodes of an electric network are connected to the poles of a battery, this results in voltages across all edges. The voltages in turn induce currents across the edges (current = voltage divided by resistance). Currents may also flow into or out of a node from or to the external battery (often referred to simply as the “exterior”).

Rücker [2012]’s analogy between NMA and electrical networks is based on the observation that resistors in parallel and sequential circuits combine in the same way as variance in pairwise and indirect meta-analysis. Variance therefore corresponds to resistance. Rücker used this connection to show that the graph theoretical methods used to derive voltages across edges in an electrical network can be used to calculate network estimates of relative treatment effects in NMA.

In Davies et al. [2022] we extended this analogy and proved that the aggregate hat matrix has an interpretation in terms of electrical current. More precisely, the elements in the row of the hat matrix corresponding to the comparison of treatments j and k can be obtained as follows: Connect a battery to nodes v_j and v_k in the electrical circuit so that one unit of current flows from the exterior into node v_j , and out of the network (to the exterior) from node v_k . The external currents into/out of all other nodes are zero. This set-up induces currents across the edges in the network. The analogy is then as follows: the current along edge $[v_l, v_m]$ is identical to the hat matrix element $H_{\perp,lm}^{(jk)}$. Further details, examples and a mathematical proof can be found in Davies et al. [2022].

The proof uses Ohm’s law and Kirchoff’s law to write the currents flowing through each edge in terms of the currents at the nodes. We define a matrix of edge currents I_\perp and a matrix of nodal currents J_\perp such that each column represents a different placement of the battery. That is, columns $I_{\perp,jk}$ and $J_{\perp,jk}$ represent the scenario in which a battery is attached across nodes v_j and v_k (with one unit of current flowing into v_j and out of v_k). The

element $I_{\perp,jk}^{(lm)}$ is then the current flowing along edge $[v_l, v_m]$ and element $J_{\perp,jk}^{(l)}$ is the current flowing from the exterior to node v_l . Nodal currents are defined as follows:

$$J_{\perp,jk}^{(l)} = \begin{cases} 1 & \text{if } l = j \\ -1 & \text{if } l = k \\ 0 & \text{otherwise.} \end{cases} \quad (\text{D.6})$$

We specify both matrices \mathbf{I}_{\perp} and \mathbf{J}_{\perp} with $N - 1$ columns such that each placement of the battery is between node v_1 one other (v_j ; $j = 2, \dots, N$). Matrix \mathbf{I}_{\perp} has K_{\perp} rows representing each edge in the unipartite graph and \mathbf{J}_{\perp} has N rows representing each node (treatment). Based on this construction, we find $\mathbf{J}_{\perp} = \mathbf{C}'_N$, where we recall $\mathbf{C}_N = [-\mathbf{1}_{N-1} \ \mathbf{I}_{N-1}]$.

The laws of electrical network theory lead to the following equation relating the edge and nodal currents,

$$\mathbf{I}_{\perp} = \mathbf{R}_{\perp}^{-1} \mathbf{B}_{\perp} (\mathbf{B}'_{\perp} \mathbf{R}_{\perp}^{-1} \mathbf{B}_{\perp})^+ \mathbf{J}_{\perp}, \quad (\text{D.7})$$

where \mathbf{B}_{\perp} is the (oriented) edge-vertex incidence matrix of the (unipartite) graph and \mathbf{R}_{\perp} is a diagonal matrix containing the resistance associated with each edge. Based on R  cker's analogy, the resistance in each edge of the electrical network is equal to the variance of the direct estimate associated with each edge in the unipartite NMA graph. Therefore, the inverse of the matrix of resistances is equal to the inverse-variance weight matrix of the aggregate model, $\mathbf{R}_{\perp}^{-1} = \mathbf{W}_{\perp}$. In Davies et al. [2022] we used this equivalence, along with $\mathbf{J}_{\perp} = \mathbf{C}'_N$ noted above, to obtain the transpose of the matrix of edge currents,

$$\mathbf{I}'_{\perp} = \mathbf{J}'_{\perp} ((\mathbf{B}'_{\perp} \mathbf{R}_{\perp}^{-1} \mathbf{B}_{\perp})^+)' \mathbf{B}'_{\perp} (\mathbf{R}_{\perp}^{-1})' \quad (\text{D.8})$$

$$= \mathbf{C}_N (\mathbf{B}'_{\perp} \mathbf{W}_{\perp} \mathbf{B}_{\perp})^+ \mathbf{B}'_{\perp} \mathbf{W}_{\perp}, \quad (\text{D.9})$$

which is equal to the aggregate hat matrix in Equation (11).

D.1.2. Random walks and electrical networks

The relationship between random walks and electrical networks is well known (Doyle and Snell [1984]). For reference, see Davies et al. [2022] (Section 4.2 and Supplementary Material Section F). We summarize the key points here.

Starting from an electrical network with resistances $R_{\perp,jk}$ along each edge, a random walk can be constructed by setting the probability of hopping from node v_j to node v_k proportional to the inverse of the resistance in edge $[v_j, v_k]$. Electrical current can then be interpreted in the random-walk picture as follows: When a voltage is applied between two nodes a and b such that the total current flowing into a and out of b from the exterior is 1, the current induced in each edge, $[v_j, v_k]$, is equal to the expected net number of times a random walker, starting at a and walking until it reaches b , moves along the edge from v_j to v_k . The net number of times the walker moves from v_j to v_k is the number of crossings in the direction from v_j to v_k minus the number of crossings in the opposite direction.

This analogy, along with the result in Equation (D.9), is the basis for Theorem 1 in the main paper.

D.2. Extension to the bipartite framework

D.2.1. NMA and electrical networks

The electrical network and random walk analogy extends easily to the bipartite framework. For an electrical network, the distinction between top and bottom nodes is not important. The bipartite graph can be treated simply as a unipartite graph with $N + M$ nodes and $K_{\perp\perp}$ edges. As before, each edge has an associated resistance. In the NMA context, edges now correspond to the arms of trials meaning the resistance in each edge is equal to the variance associated with each trial arm. Therefore, we define an $K_{\perp\perp} \times K_{\perp\perp}$ diagonal matrix of resistances \mathbf{R} with diagonal elements equal to $\sigma_{i,j}^2 + \frac{\tau^2}{2}$. We retain the notation from the main paper that i indexes trials (top nodes), while j, k, l, m refer to treatments (bottom nodes).

Next, we define the matrix of edge currents, \mathbf{I} , and the matrix of nodal currents, \mathbf{J} , for the bipartite graph. As before, we set the number of columns to $N - 1$ representing a battery attached across pairs of treatment nodes, v_1

and $v_j; j = 2, \dots, N$. Now, matrix I has K_{\perp} rows representing each edge in the bipartite graph and J has $N + M$ rows representing both the treatment and trial nodes. For a battery attached to nodes v_j and v_k , the current is +1 at node v_j , -1 at v_k , and 0 at every other treatment node ($v_l; l \neq j, k$) and every trial node ($u_i; i = 1, \dots, M$). The first M rows of J represent trial nodes which are always associated with zero current. The remaining N rows represent treatments whose value of current depends on the placement of the battery (in the same way as the unipartite framework). Therefore, we can write $J = [\mathbf{0}_{M \times (N-1)} \ C'_N]'$ where $\mathbf{0}_{M \times (N-1)}$ is an $M \times (N - 1)$ matrix of zeroes. An example of this matrix is shown in Section E.

Ohm's law and Kirchoff's law apply in the same way as before leading to the expression

$$I = R^{-1} B_{\perp\perp} (B'_{\perp\perp} R^{-1} B_{\perp\perp})^+ J, \quad (\text{D.10})$$

which depends on the (oriented) edge-vertex incidence matrix of the *bipartite* graph, $B_{\perp\perp}$. Matrix I has dimensions $K_{\perp\perp} \times (N - 1)$; each element $I_{jk}^{(il)}$ (row il and column jk) is the current flowing through edge $[u_i, v_l]$ when a battery is attached to nodes v_j and v_k . The arm-level hat matrix, on the other hand, has dimensions $(N - 1) \times K_{\perp\perp}$ with rows representing treatment comparisons and columns representing edges. To compare these matrices, we require the transpose of I ,

$$I' = J' ((B'_{\perp\perp} R^{-1} B_{\perp\perp})^+)' B'_{\perp\perp} (R^{-1})'. \quad (\text{D.11})$$

From the definition of a pseudo-inverse it is possible to show (Stoer and Bulirsch [2002]) that $(A^+)' = (A')^+$ for a general matrix A . Using this, and the fact that matrices R and $L = B'_{\perp\perp} R^{-1} B_{\perp\perp}$ are symmetric ($(R^{-1})' = R^{-1}$ and $L' = L$), we find

$$I' = J' (B'_{\perp\perp} R^{-1} B_{\perp\perp})^+ B'_{\perp\perp} R^{-1}, \quad (\text{D.12})$$

which is the result given in Equation (28) in the main paper.

D.2.2. Random walks and electrical networks

The random walk on the electrical network can be constructed in the same way as before by defining transition probabilities proportional to the inverse of the resistance in each edge. That is, the probability of hopping from one node to another is proportional to the inverse of the resistance (variance) associated with the edge connecting the two nodes, normalised with respect to the weighted degree of the first node. Since there are no edges between nodes of the same type, the walker can only hop from trial to treatment or from treatment to trial. These probabilities therefore take the same definition as those of the higher order random walk (HoRW) defined in Section 5.2.2 of the main text.

Without the NMA interpretation of the nodes and edges, the electrical network and random walk defined on this graph have the same properties as before. The differences are: (i) that edges only appear between trial nodes u_i and treatment nodes v_j , and (ii) we only consider battery placements between two treatment nodes (since our interest focuses on comparisons between treatments). The analogy can then be written as follows: When a voltage is applied between two (treatment) nodes a and b such that the total current flowing into a and out of b from the exterior is 1, the current induced in edge $[u_i, v_j]$ is equal to the expected net number of times a random walker, starting at a and walking until it reaches b , moves along the edge from u_i to v_j .

This analogy relates the bipartite edge currents $I_{jk}^{(il)}$ to the movement of a random walker. Conjecture 1 proposes an equivalent random walk interpretation for the elements of the arm-level hat matrix $H_{\perp\perp, il}^{(jk)}$. Therefore, to prove the conjecture it suffices to show that I' in Equation (D.12) is equal to the arm-level hat matrix in Equation (9) in the main text.

E. Application

In the following we present various matrices calculated for the psoriasis dataset described in Section 2 of the main text. In calculating these matrices, we order the treatments and trials alphabetically such that $(v_1, \dots, v_7) = (\text{ETN}, \text{IXE_Q2W}, \text{IXE_Q4W}, \text{PBO}, \text{SEC_150}, \text{SEC_300}, \text{UST})$ for treatments and $(u_1, \dots, u_9) = (\text{CLEAR}, \text{ERASURE}, \text{FEATURE}, \text{FIXTURE}, \text{IXORA-S}, \text{JUNCTURE}, \text{UNCOVER-1}, \text{UNCOVER-2}, \text{UNCOVER-3})$ for trials. Treatment ETN was used as the baseline and we chose a common effect (CE) model throughout. We order pairwise combinations of treatments according to the convention $([v_1, v_2], [v_1, v_3], \dots, [v_1, v_N], [v_2, v_3], [v_2, v_4], \dots, [v_2, v_N], \dots, [v_{N-1}, v_N])$. We order treatment-trial combinations according to the convention $([u_1, v_2], \dots, [u_1, v_N], [u_2, v_1], \dots, [u_2, v_N], \dots, [u_M, v_1], \dots, [u_M, v_N])$.

E.1. Conjecture 1

E.1.1. Arm-level hat matrix

The psoriasis dataset involves $M = 9$ trials, $N = 7$ treatments and $K_{\top\perp} = 28$ arms. Each arm is associated with a measure of the log odds of achieving a 75% improvement on the PASI scale. We collect these observations in the vector μ . Each n_i -armed trial is associated with $n_i - 1$ relative treatment effects measured as log odds ratios. We collect these in the vector y . The vector μ has length 28 and y has length $\sum_{i=1}^M (n_i - 1) = 19$. These two vectors are related via the 19×28 matrix C according to Equation (2). The variances and covariances associated with the log odds ratio measurements are contained in the 19×19 matrix Σ . In the CE model the weight matrix is given by its inverse, $W = \Sigma^{-1}$. The design matrix X describes which treatment comparisons appear in each trial and has dimensions 19×6 . All of these vectors and matrices are presented on page 6 alongside the resulting trial-level hat matrix, H , obtained via Equation (6) in the main text, and the arm-level hat matrix $H_{\top\perp}$ obtained via Equation (9).

E.1.2. Matrix of nodal currents

To check Conjecture 1 for the psoriasis example, we verify that the arm-level hat matrix is the same as the matrix of nodal currents calculated via Equation (28) in the main paper. This calculation requires the oriented edge-vertex incidence matrix of the bipartite graph, $B_{\top\perp}$, the matrix of edge resistances, R , and the matrix of edge currents, J . For the psoriasis network, $B_{\top\perp}$ has $N + M = 16$ columns and $K_{\top\perp} = 28$ rows. The 28×28 matrix of resistances, R , contains on its diagonal the arm-level variances associated with each log odds measurement in μ . The matrix of edge currents has dimensions 6×16 . Each of these matrices, along with the resulting matrix of nodal currents, I' , are shown on page 7.

Comparing each element of I' with the corresponding element of $H_{\top\perp}$ gives a maximum difference of 2.44×10^{-15} . Therefore, for the psoriasis example, these two matrices are identical within machine precision.

[illegible]

E.2. Conjecture 2

E.2.1. Transition matrices for the bipartite random walk

To define the random walk on the bipartite graph, we require the weighted biadjacency matrix \mathbf{B} defined in Equation (23) in the main text. For the psoriasis data, \mathbf{B} has dimensions 9×7 . Each element B_{ij} is equal to the inverse variance associated with the arm represented by edge $[u_i, v_j]$ in the bipartite graph. The downwards transition matrix \mathbf{P}^\downarrow has dimensions 9×7 . Each row i contains the probabilities of hopping from trial (top) node u_i to each of the treatment (bottom) nodes. The upwards transition matrix \mathbf{P}^\uparrow , on the other hand, describes transitions from treatments to trials and its dimensions are reversed (7×9). The inner product of the up and down transition matrices yields the 7×7 two-step transition matrix \mathbf{P} . Each element P_{jk} describes the probability of hopping between two treatment nodes, v_j to v_k , in two consecutive steps on the bipartite graph. We obtain the renormalised two-step transition matrix $\tilde{\mathbf{P}}$ by setting the diagonal elements equal to zero and renormalising the remaining probabilities in each row. All of these matrices are shown on page 9.

E.2.2. Transition matrix for the unipartite random walk

The unipartite graph of the psoriasis dataset has $K_\perp = 13$ edges and is described by the 13×7 oriented incidence matrix \mathbf{B}_\perp . Performing the aggregate model on the psoriasis data set yields a diagonal 13×13 weight matrix \mathbf{W}_\perp where each diagonal element contains the aggregate weight associated with that edge. The resulting aggregate hat matrix \mathbf{H}_\perp has dimensions 6×13 . Each row j of \mathbf{H}_\perp defines an evidence flow network from the baseline (v_1 : ETN) to treatment node v_j . The transition matrix of the random walk on the unipartite graph, \mathbf{T} , has dimensions 7×7 and is calculated via Equation (19) in the main paper. Each row describes the probability of hopping from one treatment node to each of the others. All of these matrices are shown on page 9.

Conjecture 2 is fulfilled if \mathbf{T} is equal to the renormalised two-step transition matrix $\tilde{\mathbf{P}}$. Comparing each element of these matrices yields a maximum absolute difference of 1.33×10^{-15} . Therefore, for the psoriasis example these two matrices are identical within machine precision.

$$\begin{aligned}
 B &= \begin{pmatrix} 0 & 0 & 0 & 0 & 0 & 27.309 & 55.395 \\ 0 & 0 & 0 & 10.963 & 49.448 & 36.752 & 0 \\ 0 & 0 & 0 & 0.496 & 12.555 & 11.218 & 0 \\ 79.730 & 0 & 0 & 15.661 & 72.385 & 57.073 & 0 \\ 0 & 6.586 & 0 & 0 & 0 & 0 & 26.905 \\ 0 & 0 & 0 & 2.398 & 12.223 & 6.942 & 0 \\ 0 & 37.122 & 65.202 & 21.327 & 0 & 0 & 0 \\ 85.494 & 27.432 & 60.492 & 4.379 & 0 & 0 & 0 \\ 94.656 & 34.244 & 47.092 & 16.731 & 0 & 0 & 0 \end{pmatrix} \\
 P^I &= \begin{pmatrix} 0 & 0 & 0 & 0 & 0 & 0.330 & 0.670 \\ 0 & 0 & 0 & 0.113 & 0.509 & 0.378 & 0 \\ 0 & 0 & 0 & 0.020 & 0.517 & 0.462 & 0 \\ 0.355 & 0 & 0 & 0.070 & 0.322 & 0.254 & 0 \\ 0 & 0.197 & 0 & 0 & 0 & 0 & 0.803 \\ 0 & 0 & 0 & 0.111 & 0.567 & 0.322 & 0 \\ 0 & 0.300 & 0.527 & 0.172 & 0 & 0 & 0 \\ 0.481 & 0.154 & 0.340 & 0.025 & 0 & 0 & 0 \\ 0.491 & 0.178 & 0.244 & 0.087 & 0 & 0 & 0 \end{pmatrix} \\
 P &= \begin{pmatrix} 0.446 & 0.115 & 0.201 & 0.061 & 0.099 & 0.078 & 0 \\ 0.285 & 0.216 & 0.354 & 0.095 & 0 & 0 & 0.050 \\ 0.302 & 0.216 & 0.385 & 0.097 & 0 & 0 & 0 \\ 0.221 & 0.140 & 0.234 & 0.109 & 0.170 & 0.127 & 0 \\ 0.175 & 0 & 0 & 0.083 & 0.422 & 0.319 & 0 \\ 0.145 & 0 & 0 & 0.065 & 0.336 & 0.322 & 0.131 \\ 0 & 0.064 & 0 & 0 & 0 & 0.222 & 0.713 \end{pmatrix} \\
 P^{\dagger} &= \begin{pmatrix} 0 & 0 & 0 & 0.307 & 0 & 0 & 0 & 0.329 & 0.364 \\ 0 & 0 & 0 & 0 & 0.062 & 0 & 0.352 & 0.260 & 0.325 \\ 0 & 0 & 0 & 0 & 0 & 0 & 0.377 & 0.350 & 0.273 \\ 0 & 0.152 & 0.007 & 0.218 & 0 & 0.033 & 0.296 & 0.061 & 0.233 \\ 0 & 0.337 & 0.086 & 0.494 & 0 & 0.083 & 0 & 0 & 0 \\ 0.196 & 0.264 & 0.081 & 0.410 & 0 & 0.050 & 0 & 0 & 0 \\ 0.673 & 0 & 0 & 0 & 0.327 & 0 & 0 & 0 & 0 \end{pmatrix} \\
 \tilde{P} &= \begin{pmatrix} 0 & 0.208 & 0.363 & 0.110 & 0.178 & 0.141 & 0 \\ 0.363 & 0 & 0.451 & 0.122 & 0 & 0 & 0.064 \\ 0.491 & 0.351 & 0 & 0.158 & 0 & 0 & 0 \\ 0.248 & 0.157 & 0.262 & 0 & 0.191 & 0.142 & 0 \\ 0.303 & 0 & 0 & 0.144 & 0 & 0.553 & 0 \\ 0.214 & 0 & 0 & 0.097 & 0.496 & 0 & 0.194 \\ 0 & 0.224 & 0 & 0 & 0 & 0.776 & 0 \end{pmatrix} \\
 W_{\perp} &= \begin{pmatrix} 30.010 & 0 & 0 & 0 & 0 & 0 & 0 & 0 & 0 & 0 & 0 & 0 \\ 0 & 52.217 & 0 & 0 & 0 & 0 & 0 & 0 & 0 & 0 & 0 & 0 \\ 0 & 0 & 15.877 & 0 & 0 & 0 & 0 & 0 & 0 & 0 & 0 & 0 \\ 0 & 0 & 0 & 25.667 & 0 & 0 & 0 & 0 & 0 & 0 & 0 & 0 \\ 0 & 0 & 0 & 0 & 20.238 & 0 & 0 & 0 & 0 & 0 & 0 & 0 \\ 0 & 0 & 0 & 0 & 0 & 37.276 & 0 & 0 & 0 & 0 & 0 & 0 \\ 0 & 0 & 0 & 0 & 0 & 0 & 10.051 & 0 & 0 & 0 & 0 & 0 \\ 0 & 0 & 0 & 0 & 0 & 0 & 0 & 5.291 & 0 & 0 & 0 & 0 \\ 0 & 0 & 0 & 0 & 0 & 0 & 0 & 0 & 16.824 & 0 & 0 & 0 \\ 0 & 0 & 0 & 0 & 0 & 0 & 0 & 0 & 0 & 12.237 & 0 & 0 \\ 0 & 0 & 0 & 0 & 0 & 0 & 0 & 0 & 0 & 0 & 9.123 & 0 \\ 0 & 0 & 0 & 0 & 0 & 0 & 0 & 0 & 0 & 0 & 0 & 46.815 \\ 0 & 0 & 0 & 0 & 0 & 0 & 0 & 0 & 0 & 0 & 0 & 18.292 \end{pmatrix} \\
 B_{\perp} &= \begin{pmatrix} -1 & 1 & 0 & 0 & 0 & 0 & 0 & 0 \\ -1 & 0 & 1 & 0 & 0 & 0 & 0 & 0 \\ -1 & 0 & 0 & 1 & 0 & 0 & 0 & 0 \\ -1 & 0 & 0 & 0 & 1 & 0 & 0 & 0 \\ -1 & 0 & 0 & 0 & 0 & 0 & 1 & 0 \\ 0 & -1 & 1 & 0 & 0 & 0 & 0 & 0 \\ 0 & -1 & 0 & 1 & 0 & 0 & 0 & 0 \\ 0 & 0 & -1 & 1 & 0 & 0 & 0 & 0 \\ 0 & 0 & 0 & -1 & 1 & 0 & 0 & 0 \\ 0 & 0 & 0 & 0 & -1 & 1 & 0 & 0 \\ 0 & 0 & 0 & 0 & 0 & -1 & 1 & 0 \\ 0 & 0 & 0 & 0 & 0 & 0 & -1 & 1 \end{pmatrix} \\
 H_{\perp} &= \begin{pmatrix} 0.478 & 0.333 & 0.079 & 0.056 & 0.054 & -0.357 & -0.110 & -0.055 & -0.024 & -0.034 & -0.021 & 0.022 & 0.055 \\ 0.191 & 0.648 & 0.077 & 0.045 & 0.038 & 0.225 & -0.015 & -0.018 & -0.127 & -0.038 & -0.027 & 0.007 & 0.018 \\ 0.149 & 0.254 & 0.313 & 0.160 & 0.124 & -0.004 & 0.148 & 0.005 & 0.250 & -0.165 & -0.124 & -0.005 & -0.005 \\ 0.066 & 0.091 & 0.099 & 0.498 & 0.246 & -0.016 & 0.041 & 0.041 & 0.075 & 0.161 & 0.054 & -0.340 & -0.041 \\ 0.080 & 0.099 & 0.097 & 0.312 & 0.412 & -0.028 & 0.035 & 0.073 & 0.071 & 0.074 & 0.130 & 0.385 & -0.073 \\ 0.169 & 0.152 & 0.093 & 0.254 & 0.332 & -0.102 & 0.002 & 0.269 & 0.050 & 0.049 & 0.096 & 0.304 & 0.731 \end{pmatrix} \\
 T &= \begin{pmatrix} 0 & 0.208 & 0.363 & 0.110 & 0.178 & 0.141 & 0 \\ 0.363 & 0 & 0.451 & 0.122 & 0 & 0 & 0.064 \\ 0.491 & 0.351 & 0 & 0.158 & 0 & 0 & 0 \\ 0.248 & 0.157 & 0.262 & 0 & 0.191 & 0.142 & 0 \\ 0.303 & 0 & 0 & 0.144 & 0 & 0.553 & 0 \\ 0.214 & 0 & 0 & 0.097 & 0.496 & 0 & 0.194 \\ 0 & 0.224 & 0 & 0 & 0 & 0.776 & 0 \end{pmatrix}
 \end{aligned}$$

F. Simulation study

F.1. Methods

F.1.1. Generating random networks of treatments and trials

Simulating NMA requires two generation procedures: (i) generating the network structure, i.e. which treatments are compared in which trials, and (ii) generating synthetic outcome data in each trial. To date, simulation studies of NMA have focused on the latter, with authors specifying the structure of their network manually before randomly sampling the outcome data from some underlying model. This first step becomes a laborious task for large networks, especially if characteristics of the network need to be varied. Therefore, simulations of NMA have tended to involve small networks (usually ≤ 5 treatments) with a limited range of geometries. To the best of our knowledge, only one study (Kanters et al. [2021]) has attempted to automate the generation of treatment-trial structures, but these networks were restricted to two-arm trials.

To effectively sample networks with multi-arm trials, we require an algorithm that generates graphs with higher-order structures. In the following, we make use of a simple algorithm for random bipartite graphs.

F.1.2. Random bipartite graphs

In random graph theory, there exist numerous algorithms for the generation of graphs. The simplest is the Erdős-Renyi (ER) model (Erdos and Renyi [1959, 1960]) where it is assumed that, for a fixed number of vertices and edges, all possible graphs are equally likely. This model extends naturally to bipartite graphs. Here, for a fixed number of top nodes N , bottom nodes M , and edges $K_{T\perp}$, every possible bipartite graph is equally likely.

The `igraph` software in R (Csardi and Nepusz [2006], Csárdi et al. [2025]) has a function `sample_bipartite` that generates bipartite graphs according to the ER model. We use this to generate random NMA graphs with N treatments, M trials, and $K_{T\perp}$ arms. To sample valid NMA networks we impose two additional restrictions: (i) every trial must contain at least two arms, and (ii) the network must be connected.

Once we have sampled a random graph using `sample_bipartite`, we ensure condition (i) is fulfilled by sampling additional arms for every trial node with degree < 2 . If a trial node has degree 0, we sample any two treatment nodes and connect them to that trial. If a trial has degree 1, we sample one additional treatment from the bottom nodes that are not already connected to that trial.

We enforce condition (ii) by using the `igraph` function `count_components` to count the number of connected components of the graph. If this number is greater than 1 then the network is disconnected. To connect it, we randomly sample two components and a bottom node from each, v_j and v_k . Next, we sample a trial node u_i from the neighbours of v_j and v_k (i.e., from all the trials that contain one of those treatments). If u_i is connected to v_j , we add a new edge connecting it to v_k . Otherwise, if u_i is connected to v_k , we add a new edge to v_j . If there are no trial nodes connected to either v_j or v_k , we sample a trial from the full set of top nodes and connect it to both.

F.1.3. Simulation set up

In our simulation, we generate 10,000 random networks using the procedure described in Section F.1.2. At each iteration we sample the number of treatments N from a uniform distribution between 3 and 50, and the number of trials M from a uniform distribution between 2 and 200. Each trial must have at least two arms, so the minimum number of total arms in the network is $2M$. The maximum number of total arms is NM , i.e. every trial involves all possible treatments. In reality, the number of arms in a trial tends to be fairly low (e.g, usually ≤ 6). Therefore, we sample the number of edges (arms) $K_{T\perp}$ from a half normal distribution bounded between $2M$ and NM with a standard deviation of $(NM - 2M)/2$. This ensures that we sample from the full range of possible arms, but gives precedence to lower numbers. Because of the additional restrictions on the network structure (see (i) and (ii) above), the final sampled network may have more arms than originally specified.

To calculate the matrices required to check the two conjectures, we need the variance associated with each trial arm. We sample these values from a half-normal distribution with a standard deviation s . For each network, we sample s uniformly between 0.5 and 2. To check Conjecture 1, we calculate $H_{T\perp}$ and I' for each network and calculate the difference between each corresponding element. For Conjecture 2, we calculate and compare each element of T and \hat{P} .

F.2. Results

Table F.1 summarizes the characteristics of the bipartite NMA graphs sampled in the simulation and their unipartite projections. We show the mean, standard deviation (SD), minimum, and maximum values of various graph metrics across the 10,000 random networks. The definitions of these metrics are given in the table footnote.

Table F.1. Characteristics of the 10,000 NMA networks sampled in the simulation.

	Mean	SD	Minimum	Maximum
Number of treatments (bottom nodes), N	26.7	13.9	3	50
Number of trials (top nodes), M	99.7	57.6	2	200
Number of edges in the bipartite graph (arms), $K_{T\perp}$	1097.4	1173.1	5	8853
Number of edges in the unipartite graph, K_{\perp}	397.8	352.2	3	1225
Degree of top nodes: mean	11.1	8.6	2.1	49.5
minimum	6.8	7.2	2	48
maximum	16.0	9.7	3	50
Degree of bottom nodes: mean	44.3	37.1	1.0	191.8
minimum	36.8	35.4	1	187
maximum	52.1	38.7	2	195
Degree of unipartite nodes: mean	23.4	13.5	2	49
minimum	21.4	13.9	1	49
maximum	24.8	13.5	2	49
Density of the bipartite graph	0.45	0.23	0.05	1.00
Density of the unipartite graph	0.93	0.17	0.10	1.00
Radius of the unipartite graph	1.14	0.39	1	6
Mean distance of the unipartite graph	1.08	0.24	1.00	4.80

The density of a graph is the ratio of the number of edges to the number of possible edges. A density of 1 means the network is fully connected. The distance between two vertices is the minimum number of edges between them. The eccentricity of a node is the maximum distance from that node to any other. The radius of a graph is the minimum eccentricity of any node in the graph. In NMA, the degree of a top node (trial) in the bipartite graph is the number of arms in that trial. The degree of a bottom node (treatment) corresponds to the number of trials that treatment is involved in. The degree of a treatment node in the unipartite graph is the number of other treatments that treatment has been directly compared to.

Conjecture 1:

Across all 10,000 networks, the maximum difference between any two corresponding elements of $H_{T\perp}$ and I' was 6.03×10^{-11} . Therefore, Conjecture 1 holds (within machine precision) for all sampled networks.

Conjecture 2:

Across all 10,000 networks, the maximum difference between any two corresponding elements of T and \tilde{P} was 1.15×10^{-13} . Therefore, Conjecture 2 holds (within machine precision) for all sampled networks.